

**Application of a Model to Predict Algal Behaviour in Rivers at  
Ömerli Reservoir, Turkey**

**by**

**Sevil Kahraman Özen**

**B.S. Fisheries Engineering, Fisheries Faculty, İstanbul University, 2006**

**B.S. Business Administration, Anadolu University, 2009**

**Submitted to the Institute of Environmental Sciences in partial fulfillment of  
the requirements for the degree of**

**Master of Science**

**in**

**Environmental Sciences**

**Boğaziçi University**

**2014**

## ACKNOWLEDGEMENTS

I would like to express my sincere gratitude and deep regards to Assist. Prof. Başak Güven, my advisor, for her professional knowledge, all constant guidance, and patience with this thesis, which helped me in completing this study through various stages.

I would like to express my kindly profound regards to Assoc. Prof. Raşit Bilgin and Assoc. Prof. Melike Gürel for being in my thesis committee and for their valuable comments and contributions to my study.

I also take this opportunity to express a deep sense of gratitude to Prof. Dr. Mustafa Temel and Assist. Prof. Ali Serhan Tarkan for providing valuable datasets to carry out my studies.

I would also like to thank to Boğaziçi University Research Fund for supporting this study with the project code 14Y00P5.

My grateful thanks also extended to Mr. Serkan Kaptan for his help in doing site figures and Ms. Arin Küçükdoğan for calculating GIS fields results.

Finally, I wish to thanks to my family for their priceless support and encouragement throughout my life.

## ABSTRACT

The occurrence of small populations of algal blooms in lakes, reservoirs, rivers and other freshwater environments is natural. However, under favourable conditions, the population size can increase dramatically and the algae may accumulate at the freshwater surface as a concentrated bloom. As a result of the bloom occurrence, water resources and water-body users can face the problems of reduced aesthetic quality, emission of unpleasant odours, blocking of water-filtration systems and release of toxins into the water. The apparent increase in the frequency of bloom events is a symptom of eutrophication, and requires monitoring and management. Numerous modelling studies have been carried out to predict the behaviour of algae in freshwaters. However, in Turkey, modelling studies regarding algal growth or transport have rather been limited, particularly in river systems. The main objective of the study is to provide predictions about the intensity, timing and location of the potential algal blooms in selected streams of the Ömerli Reservoir. In order to achieve this, a formerly developed deterministic-mathematical model is applied to the selected streams of the Ömerli Reservoir. Monthly field data obtained from 3 different streams of the reservoir, for 1 year is used as input data for the model application. Results indicated that the model predictions are quite reasonable in terms of expressing the relationships between environmental conditions such as, irradiance, nutrient, temperature, turbulence, and algal density change. Furthermore, the simulations also indicate an acceptable prediction of seasonal chl-*a* concentrations. As a result of this study, it can be said that the model simulation results fit reasonably well with the findings in the literature.

## ÖZET

Algal bloom, mikroskobik su yosunlarındaki (Algler) büyüme ve artışlarla göl, rezervuar, dere gibi tatlı sularda küçük populasyonlar halinde görülen doğal bir çevre olayıdır. Elverişli şartlar oluştuğunda, alg populasyonu hızlı bir şekilde artarak, tatlı su yüzeylerinde birikerek alg tabakalaşmalarına sebep olur. Algal tabakalarının oluşumuyla birlikte, su kaynakları ve su kaynakları kullanıcıları; azalmış estetik kalite, hoş gitmeyen kötü koku emisyonları, su filtre sistemlerinin tıkanması, ve toksik içeriğin suya serbest bırakılması gibi problemlerle karşılaşabilir. Alg artışı olaylarının sık görülmesi ötrofikasyon göstergesi olup, su kaynaklarının ve havzaların doğru ve etkin bir şekilde yönetimini gerektirir. Tatlı sularda alg davranışının tayinine yönelik tahminlerde bulunabilmek için birçok modelleme çalışmaları yapılmaktadır. Buna rağmen, Türkiye’de, özellikle akarsu sistemlerinde, alglerin büyümesi ve taşınması konusunda, yapılan modelleme çalışmaları kısmen kısıtlıdır. Bu çalışmanın asıl amacı, Ömerli rezervuarından seçilmiş üç farklı dereden bir yıllık süre ile aylık alınan saha verilerinin model datası olarak, önceden geliştirilmiş matematiksel bir modele uygulanarak, potansiyel alg tabakalaşmalarının yoğunluğunu, lokasyonunu ve zamanlamasını tahmin etmektir. Model sonuçları, besin, ışık, sıcaklık ve türbülans gibi çevresel şartların değişimi ile değişen alg yoğunluk ve miktarı arasındaki ilişkiyi tahmin etmek konusunda oldukça makul sonuçlar göstermiştir. Simülasyon sonuçları ayrıca, mevsimsel Chl-*a* değişimlerinin kabul edilebilir tahminlerine işaret etmektedir. Özetleyecek olursak, model simülasyon sonuçları literatürdeki bulgular ile oldukça uyumlu olduğu söylenebilir.

## TABLE OF CONTENTS

ACKNOWLEDGMENTS	iii
ABSTRACT	iv
ÖZET	v
TABLE OF CONTENTS	vi
LIST OF FIGURES	vii
LIST OF TABLES	xi
LIST OF SYMBOLS/ABBREVIATIONS	xii
1. INTRODUCTION	1
2. BACKGROUND	3
3. METHODOLOGY	12
3.1. Site Description	12
3.2. Model Description	14
3.3. Data Requirements	19
3.3.1. Topographical Data	20
3.3.2. River Quality Data	23
4. RESULT AND DISCUSSIONS	27
4.1. Verification of the Model	27
4.2. Results of the Growth Model	31
4.2.1. Effect of Day Length on Colony Growth	31
4.2.2. Effect of Irradiance on Colony Growth	32
4.2.3. Effect of Nutrient limitation on Colony Growth	36
4.3. Results of Movement Model	41
4.4. Simulated vs. Measured Chl- <i>a</i> Results	44
5. CONCLUSIONS AND RECOMMENDATIONS	48
REFERENCES	50
APPENDIX A	58
APPENDIX B	67

## LIST OF FIGURES

Figure 2.1.	Diagram summarizing the possible sequence of events in buoyancy regulation by algae	4
Figure 3.1.	Illustration of Riva, Paşaköy, and Kömürlük Rivers in the Ömerli Reservoir	13
Figure 3.2.	The topographical map of the Ömerli Reservoir catchment area	13
Figure 3.3.	A screenshot of the computer simulation program showing the ‘Edit Parameters’ menu	17
Figure 3.4.	A schematic representation of information flow	18
Figure 3.4.	Elevation map of the Ömerli Reservoir	21
Figure 3.6.	Slope map of the Ömerli Reservoir	21
Figure 3.7.	Flow direction map of the Ömerli Reservoir	22
Figure 3.8.	Flow accumulation of the Ömerli Reservoir	22
Figure 4.1.	Simulation of colony density for the Kömürlük River: Reach 2	29
Figure 4.2.	Simulation of colony density for the Paşaköy River: Reach 2	29
Figure 4.3.	Simulation of colony density for the Riva River: Reach D and Reach C	29

Figure 4.4.	Simulation of colony depth for the K�m�rl�k River: Reach 2	30
Figure 4.5.	Simulation of colony depth for the Pařak�y River: Reach 1	30
Figure 4.6.	Simulation of colony depth for the Pařak�y River: Reach 2	31
Figure 4.7.	Simulation of colony density for the Riva River Reach 1, Reach 2	32
Figure 4.8.	Simulation of colony density for the K�m�rl�k River: Reach 2	33
Figure 4.9.	Simulation of colony density for the Pařak�y River: Reach 1	34
Figure 4.10.	Simulation of colony density for the Riva River: Reach 1,2,G, F, and E	34
Figure 4.11.	Simulation of colony density for the Riva River: Reach B and A	35
Figure 4.12.	Simulation of colony density for the Riva River: Reach D and C	35
Figure 4.13.	The effect of minimum nutrient conditions on colony growth in K�m�rl�k River	37
Figure 4.14.	The effect of maximum nutrient conditions on colony growth in K�m�rl�k River	38

Figure 4.15.	Simulation of colony density for the Riva River: Reach 2 under low nutrient conditions	38
Figure 4.16.	Simulation of colony density for the Riva River: Reach 2 under high nutrient conditions	39
Figure 4.17.	Simulation of colony density for the Paşaköy River: Reach 1 under low nutrient conditions	40
Figure 4.18.	Simulation of colony density for the Paşaköy River: Reach 1 under high nutrient conditions	40
Figure 4.19.	Simulation of colony depth for the Riva River: Reach 1	41
Figure 4.20.	Simulation of colony depth for the Riva River: Reach 1	42
Figure 4.21.	Simulation of colony depth for the Kömürlük River: Reach 1	43
Figure 4.22.	Simulation of colony depth for the Riva River: (a) Reach A (b) Reach G	43
Figure 4.23.	Simulation of Chl- <i>a</i> for the Kömürlük River: Reach1	44
Figure 4.24.	Simulation of Chl- <i>a</i> for the Paşaköy River: Reach 1	44
Figure 4.25.	Simulation of Chl- <i>a</i> for the Paşaköy River: Reach 1	45
Figure 4.26.	Measured Chl- <i>a</i> for the Paşaköy River: Reach 1	45
Figure 4.27.	Simulated vs. Measured Chl- <i>a</i> concentrations for the Kömürlük River	47

Figure A.1.	A screenshot of the computer simulation program showing the ‘Variables’ menu for Riva River Reach 1.	58
Figure A.2.	A screenshot of the computer simulation program showing the ‘Parameters’ menu for the Riva River, Reach 1.	59
Figure A.3.	A screenshot of the computer simulation program showing the ‘Monthly Data’ menu for the Riva River, Reach 1.	60
Figure A.4.	A screenshot of the computer simulation program showing the ‘Variables’ menu for the Paşaköy River, Reach 1.	61
Figure A.5.	A screenshot of the computer simulation program showing the ‘Parameters’ menu for the Paşaköy River, Reach 1.	62
Figure A.6.	A screenshot of the computer simulation program showing the ‘Monthly Data’ menu for the Paşaköy River, Reach 1.	63
Figure A.7.	A screenshot of the computer simulation program showing the ‘Variables’ menu for the Kömürlük River, Reach 1.	64
Figure A.8.	A screenshot of the computer simulation program showing the ‘Parameters’ menu for the Kömürlük River, Reach 1.	65
Figure A.9.	A screenshot of the computer simulation program showing the ‘Monthly Data’ menu for the Kömürlük River, Reach 1.	66
Figure B.1.	Flowchart of the computer simulation program.	67

## LIST OF TABLES

Table 2.1.	General features of the cyanotoxins	7
Table 2.2.	History of algal behaviour models: A chronological and cross-sectional representation	10
Table 3.1.	The model variables	19
Table 3.2.	Summary of the river quality data that is used in the model	23
Table 3.3.	Physical, Chemical and Biological data of Riva River	23
Table 3.4.	Physical, Chemical and Biological characteristics of the Riva River data	24
Table 3.5.	Physical, Chemical and Biological characteristics of the Paşaköy River data	25
Table 3.6.	Physical, chemical and biological characteristics of the Kömürlük River Data	26
Table 4.1.	Data of the Kömürlük River is used in the model	28

## LIST OF SYMBOLS/ABBREVIATIONS

Symbol	Explanation	Units used
Chl- <i>a</i>	Chloropyll- <i>a</i>	( $\mu\text{g l}^{-1}$ )
CSTR	Continuously Stirred Tank Reactors	
DO	Dissolved Oxygen	( $\text{mg l}^{-1}$ )
<i>g</i>	gravitational acceleration	( $\text{m s}^{-1}$ )
GIS	Geographical Information Systems	
$K_N$	half saturation constants for N	
$K_P$	half saturation constants for P	
N	Nitrogen	
$\text{NH}_4$	Ammonia	
$\text{NO}_2\text{-N}$	Nitrite	( $\mu\text{g l}^{-1}$ )
$\text{NO}_3\text{-N}$	Nitrate	( $\text{mg l}^{-1}$ )
<i>o</i> - $\text{PO}_4$	orthoPhosphate	( $\mu\text{g l}^{-1}$ )
P	Phosphorus	
pH	Potential Hydrogen	
$\text{SiO}_2$	Silicon dioxide	( $\text{mg l}^{-1}$ )
SSP	Suspended Solid Particule	( $\text{mg l}^{-1}$ )
$\text{SO}_4$	Sulphate	( $\text{mg l}^{-1}$ )
TDS	Total Dissolved Solids	( $\text{mg l}^{-1}$ )
TN	Total Nitrogen	
TP	Total Phosphorous	( $\mu\text{g l}^{-1}$ )
<i>a</i>	the algal biomass concentration and is directly proportional to the concentration of chlorophyll- <i>a</i> ( $\text{mg l}^{-1}$ )	
<i>A</i>	proportion of cell volume relative to colony volume	
$C_0$	a constant	
$c_1$	rate coefficient determining the increase in density with time	( $\text{kg m}^{-3} \text{min}^{-1}$ )
$c_2$	light-dependent rate coefficient describing the decrease in density with time	( $\text{kg m}^{-3} \text{min}^{-1}$ )
$c_3$	the minimal rate of density decrease	( $\text{kg m}^{-3} \text{min}^{-1}$ )

$d$	river depth	
$dt$	in time	
$d\rho/dt$	change in density with time	( $\text{kg m}^{-3} \text{ min}^{-1}$ )
$du/dz$	velocity gradient	
$l$	characteristic length known as the mixing length	
$\bar{I}_z$	average irradiance	( $\mu\text{mol m}^{-2} \text{ s}^{-1}$ )
$I_a$	previous irradiance	
$K_1$	irradiance at which the rate of density increase with time is half the maximal rate	( $\mu\text{mol m}^{-2} \text{ s}^{-1}$ )
$\mathcal{K}$	von Karman's universal constant	
$k_d$	death rate	( $\text{d}^{-1}$ )
$n$	viscosity of the water	( $\text{kg m}^{-1} \text{ s}^{-1}$ )
$n_{\text{roughness}}$	Manning's roughness coefficient	
$P$	time step	(min)
$Q$	flow	( $\text{l s}^{-1}$ )
$R$	channel's hydraulic radius	(m)
$r$	effective radius of the colony	(m)
$S_e$	slope of the channel's energy grade line	
$u$	mean river velocity	( $\text{m s}^{-1}$ )
$ u' $	absolute values of the instantaneous lateral turbulent velocity fluctuations	( $\text{m s}^{-1}$ )
$u(z)$	velocity profile	( $\text{m s}^{-1}$ )
$u^*$	shear velocity	( $\text{m s}^{-1}$ )
$V$	control volume	( $\text{m}^3$ )
$ w' $	the absolute values of the instantaneous vertical turbulent velocity fluctuations	( $\text{m s}^{-1}$ )
$z$	distance from the water surface	(m)
$z_0$	height where velocity is zero	(m)

$\phi$	form resistance	
$\rho$	colony density	(kg m <sup>3</sup> )
+	temperature-activity coefficient	

## 1. INTRODUCTION

The occurrence of small populations of algae in lakes, reservoirs, rivers and other freshwater environments is natural. However, under favourable conditions for algal growth, the population can increase dramatically and the algae may accumulate at the freshwater surface as a concentrated bloom. As a result of the bloom occurrence, water resources and water-body users can face the problems of;

- reduced aesthetic quality,
- emission of unpleasant odours,
- blocking of water-filtration systems,
- release of toxins into the water.

Algal blooms can be regarded as one of the major symptoms of the global eutrophication problem. More importantly, toxins produced by some toxin producing genera of algae, particularly, cyanobacteria, have high toxicity to animals and humans. The symptoms of algal toxin poisoning can be serious. Severe poisoning incidents caused by algal bloom toxins have been reported from many countries around the world. Indeed, toxic algal blooms have probably done more to give eutrophication its bad name than any other consequence of lake enrichment.

It is important to develop both short-term and long-term action plans to manage the problem of toxic algal blooms. For example, National Rivers Authority (NRA) of England and Wales recommended that “the use of predictive models, to quantify the development of algal blooms in relation to changes in environmental variables, should be further evaluated. If necessary, further research should be initiated so that models can be used to devise management plans for different bodies of water” (NRA, 1990).

Numerous modeling studies have been carried out to predict the behaviour of algae in freshwaters. However, in Turkey, modeling of algal growth or transport have rather been limited, particularly in river systems.

The main objective of the study is to provide predictions about the intensity, timing and location of the potential algal blooms in rivers at Ömerli Reservoir. In order to achieve this, a formerly developed theoretical model (Güven and Howard, 2006b) is applied to streams at Ömerli Reservoir. Monthly water quality data obtained from three different streams of the reservoir (Temel, 2006; Tarkan, 2007; Tarkan 2010), for one year is used as input data for model application to Riva, Paşaköy and Kömürlük Streams for the prediction of algal growth.

This thesis provides a field application of a simulation model for the prediction of algal growth and colony movement. Chapter 2 outlines the problems associated with excess growth of algae, basic mechanisms governing algal density change, and formerly developed models of algal population dynamics. Chapter 3 describes the mathematical model, presents the data requirements and gives methodological approaches and tools carried out for model application. Chapter 4 presents the model simulation results and discussion. Finally, several important conclusions that can be drawn from the study presented in this thesis are outlined in Chapter 5.

## 2. BACKGROUND

Algae get their own energy from photosynthesis and can exist in terrestrial, and aquatic habitats; oceans, rivers, lakes, oil, and even bare rocks. Blue-green algae are one of the largest and most important groups of bacteria having an extensive fossil record from Archaean rocks of western Australia being more than 2.8 billion years old (Oslo, 2006).

Nuisance algal blooms reduce the aesthetic quality of water by discoloration. They also cause taste and odour problems by synthesizing low molecular weight compounds found in aquatic environments. Furthermore, algal blooms may block water filtration systems, hence cause problems for water supplies. Finally, and most importantly; algal toxins, which are produced by some toxin-producing species of the cyanobacteria genera have high toxicity to animals and humans.

In water, algae can form gas vesicles, which give an ability to colonies to float in water column. Algae can move in water column by regulating their gas vesicles and cell balast (Ibelings et al., 1991; Walsby, 1994; Sigee, 2005). Algae stay in the radiation rich upper water column to promote carbon fixation, and this result in the formation of carbohydrates as glycogen, which acts as cell balast. As a result, algae become heavier and start to sink in the water column during the day, under continous illumination. On the contrary, under reduced illumination, a decline in glycogen occurs, and that rises up the buoyancy function to run upwards for photosynthesis. Buoyancy of algae depends on the colony density in relation to the surrounding water density; therefore, the rate of density change plays an important role in the buoyancy regulation of algal cells. There are three major mechanisms to explain how the buoyant state of algae changes. These are:

- regulation of gas vesicle synthesis,
- changes in cell turgor pressure,
- production of carbohydrate ballast by photosynthesis.

A detailed illustration of this process is provided in Figure 2.1.

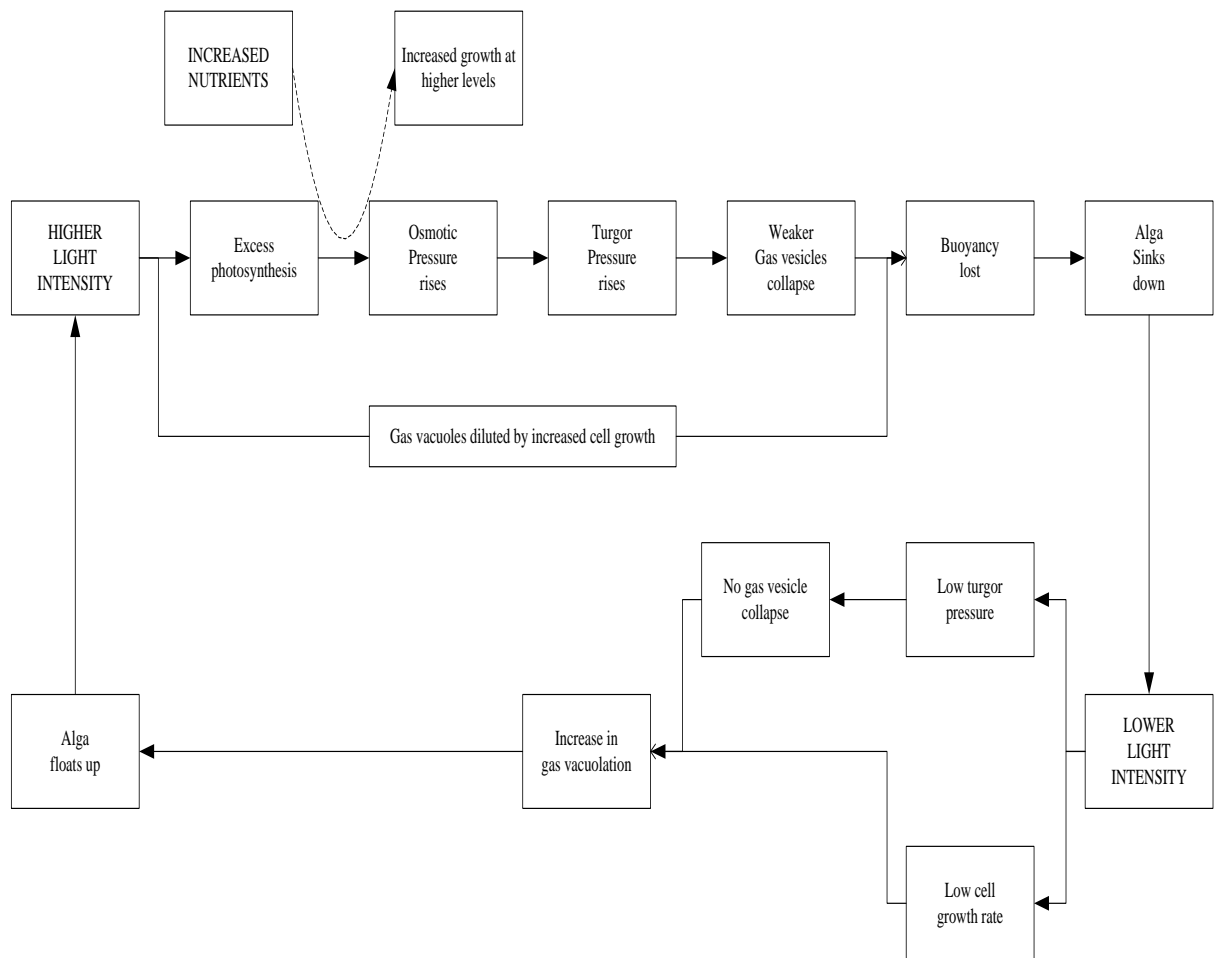


Figure 2.1. Diagram summarizing the possible sequence of events in buoyancy regulation by cyanobacteria (redrawn from Reynolds and Walsby, 1975).

The gas vesicles within cells of algae are subject to an internal osmotic pressure. This is called the cell turgor pressure. Intracellular turgor pressure increases by the osmotic potential difference between the algal cell and the surrounding medium. When hydrostatic pressure increases with increasing depth beneath the water surface, gas vesicles collapse as a result of the application of correspondingly lower external pressures (Reynolds et al., 1987). Turgor pressure rise is caused by an increase in photosynthetic activity and products (Grant and Walsby, 1977) and light stimulated uptake of potassium ions (Allison and Walsby, 1981). When turgor pressure increases beyond a certain level, gas vacuoles collapse, the cells lose buoyancy and sink through the water column. According to Walsby (1970), there is an inverse correlation between gas vacuolation and light intensity. It was first demonstrated by Walsby (1971) that an increase in light intensity causes turgor pressure to rise and weak gas vesicles in *Anabaena flos-aquae* collapse.

Due to high nutrient content, increase of mass population of algae may eventually results in eutrophication, which is a natural phenomenon. This situation may even get worse as a result of increased pollution or climate change. Under favorable conditions of light, nutrients, and temperature, water bodies may suffer from toxic algal blooms, especially in spring and midsummer. Sometimes, nuisance algal blooms can appear as blue-green sums at the water surface. Generally, there is an annual cycle for the growth of algal blooms.

In addition to the eutrophication problem, some algae, especially cyanobacteria, have high amount of toxicity to humans and animals. Algal toxins can poison fish, shellfish, birds, mammals, and humans. Cyanotoxins are known as one of the most common algal toxins produced by the algae. *Microcystis*, *Oscillatoria*, *Anabaena* and *Aphanizomenon* are the most common toxin producing genera (Codd et al., 1988). Cyanotoxins can be categorized into three main groups:

- Cyclic peptides (hepatotoxins),
- Alkaloids (neurotoxins, cytotoxins, and dermatotoxins), and
- Lipopolysaccharides.

Hepatotoxins are the most dispersed, and have main concern to human health. Microcystins cause accumulation of blood in the liver cells and death by hypovolemic shock (Falconer,1989). In 1979, a human poisoning event occurred in a hepatoxins contaminated drinking reservoir in Australia (Chorus and Bartram,1999).

Neurotoxins affect the nervous system and produced by some strains of *Anabaena*, *Aphanizomenon* and *Oscillatoria*. Neurotoxicity is related by respiratory distress, paralysis, and tremors. Death may occur rapidly within 2-30 minutes by neurotoxins in mouse (Chorus and Bartram,1999). Ingestion of the toxic cells and extracellular toxin from a water bloom causes the poisoning of animals by neurotoxins (Carmichael, 1986). Cases of poisoning in many animals have been reported in Europe, North America, and Australia. For example, sheep deaths were recorded after drinking water from a farm dam contaminated with the neurotoxic *Anabaena circinalis* in Australia (Negri *et al.*, 1995).

Dermatoxins are originated by benthic marine cyanobacteria such as *Lyngbya*, *Oscillatoria* and *Schizothrix*. Allergic reaction on skin can be seen in swimmers, irritation of skin and eyes.

Lipopolysaccharides (LPS) are considered to be produced by the outer cell wall of cyanobacteria. They are also known as irritant toxins, and they cause allergic responses in humans and animals.

General features regarding these toxin groups are given in Table 2.1.

Table 2.1. General features of the cyanotoxins (Chorus and Bartram, 1999).

	Toxin group	Primary target organ in mammals	Cyanobacterial genera
<b>Cyclic peptides</b>	Microcystins	Liver	<i>Microcystis, Anabaena, Oscillatoria, Nostoc, Hapalosiphon, Anabaenopsis</i>
	Nodularin	Liver	<i>Nodularia</i>
<b>Alkaloids</b>	Anatoxin-a	Nerve synapse	<i>Anabaena, Oscillatoria, Aphanizomenon</i>
	Anatoxin-a(S)	Nerve synapse	<i>Anabaena</i>
	Aplysiatoxins	Skin	<i>Lyngbya, Schizothrix, Oscillatoria</i>
	Cylindrospermopsins	Liver	<i>Cylindrospermopsis, Aphanizomenon, Umezakia</i>
	Lyngbyatoxin-a	Skin, gastrointestinal track	<i>Lyngbya</i>
	Saxitoxins	Nerve axons	<i>Anabaena, Aphanizomenon, Lyngbya, Cylindrospermopsis</i>
<b>LPS</b>	Lipopolysaccharides (LPS)	Potential irritant; affects any exposed tissue	All

Almost 1000 years ago, in southern China, General Zhu Ge-Ling reported that when crossing green coloured river they lost troops that drank from green water (Chorus and Bartram, 1999). Since 2001, 11 dogs died after swimming in algal bloom affected rivers in Humboldt and Mendocino Counties in the US (California Regional Water Quality Control, 2009). In 1996, in Brazil, 60 dialysis patients died after receiving toxic algae contaminated water (Pouria et al., 1998). In 1989, 20 sheep from and 15 dog died by drinking water from Rutland River in Leicestershire (UK), which is dominated by blooms of *M.aeruginosa* (Ferguson, 1997).

Eutrophication affects both environmental concern and money lost. For instance, in the UK, the cost of sewage treatment for eutrophication control was £ 950 million in the last 15 years (Kinniburgh and Barnett, 2010), and £ 75-114 million per year were spent in England and Wales for the remediation (Pretty *et al.*,2002). As a result, Water Framework Directive council of European Union put a legal pressure on to each European member country to manage their aquatic environments for sustaining better status.

It is crucial to understand the algal behaviour, especially in terms of population growth and colony transport, in order to be able to predict future bloom events, hence to manage the eutrophication problem. Process-based mathematical models may act as useful tools both for interpreting algal growth and transport mechanisms and for predicting the intensity, timing and location of bloom events (Güven and Howard, 2006b).

The value of modeling has been recognized for a number of years. Accurate and well-validated models are able to provide predictions of the behaviour of dynamically changing systems and provide data and insights that would be difficult or impossible to obtain by conventional field and laboratory methods. There are mainly two common modeling methodologies that are applied to algal behaviour modeling. These are, deterministic mathematical modelling and Artificial Neural Network modeling. Process-based models are generally developed by undertaking deterministic-mathematical approaches, whereas Artificial Neural Networks can be regarded as an empirical approach. Artificial Neural Networks are advantageous from two aspects: Firstly, no *a priori* information is required to determine the model structure or to estimate parameters. Secondly, models developed by neural networks are flexible and adaptable to alternative scenarios. The results produced from a neural network modelling approach are highly predictive; however, this technique lacks in representation and interpretation mechanisms of the algal growth and transport in freshwater systems(Güven and Howard, 2006a). For these reasons, this technique can also be regarded as the ‘black-box’ modeling. Although difficult to develop, to account for the complex relationships between the components of the freshwater ecosystems, deterministic mathematical models with process-based equations will always be required for interpretation of algal growth behaviour and algal transport mechanisms.

Therefore, use of properly calibrated and validated mathematical models that can simulate the origin, growth and demise of problem blooms has been recognized by governmental bodies and the water industry. For example, Ferguson (1997) and Reynolds and Irish (1997) have described the development of models for use by the Environment Agency in England and Wales, which offer insight and information suitable for use in development management action plans. The formulation of process-based models of buoyancy change and vertical migration in algae are being developed based on extensive laboratory work (e.g. Kromkamp and Walsby, 1990; Visser *et al.*, 1997). However, modeling techniques such as Artificial Neural Networks also indicate promising results in accurately predicting the timing and magnitude of bloom events (e.g. Maier and Dandy, 1997; Recknagel, 1997; Whitehead *et al.*, 1997). More recently, many computer simulation models have been successfully applied to various aquatic environments in order to predict blooming for changing scenarios around the world. For example, Fadel *et al.* (2011) developed a coupled hydrodynamic biological model of cyanobacteria dynamics in reservoirs, which was applied to the Grangent reservoir in France. Jöhnk *et al.* (2011) modeled the life cycle and population dynamics of *Nostocales*, and applied their model to the Lake Melangsee in Germany. Computer simulations of seasonal outbreak and diurnal vertical migration of cyanobacteria was also studied in Japan by Hiroshi *et al.* (2008).

A chronological representation of selected modeling studies from the literature regarding algal behaviour, including the modeling environment, modeled processes, and modeling technique are provided in Table 2.2.

Table 2.2. History of algal behaviour models: A chronological and cross-sectional representation (modified and updated from Guven and Howard, 2006a).

Freshwater Environment	Modeled Processes	Modeling Technique	Reference
Lake	Algal growth	Mathematical, process-based	O'Brien (1974)
Lake	Algal growth	Mathematical, process-based	Bannister (1979)
River	Phytoplankton dynamics	Mathematical, process-based	De Boer (1979)
Lake	Algal movement	Mathematical, process-based	Okada and Aiba (1983 a,b)
River	Algal growth	Mathematical, process-based	Bingham <i>et al.</i> (1984)
River	Algal growth and movement	Mathematical, process-based	Whitehead and Hornberger (1984)
River	Algal growth	Mathematical, process-based	Young <i>et al.</i> (1985)
River	Algal growth	Mathematical, process-based	Lung and Paerl (1988)
Lake	Algal growth	Mathematical, process-based	Laws and Chalup (1990)
Lake	Algal movement	Mathematical, process-based	Kromkamp and Walsby (1990)
Lake	Algal movement	Mathematical, process-based	Howard (1993)
River	Algal growth	Mathematical, process-based	Cloot and Roux (1996)
Lake	Algal movement	Mathematical, process-based	Belov and Giles (1997)
River	Algal growth	Artificial Neural Networks	Maier and Dandy (1997)
River	Species abundance	Artificial Neural Networks	Recknagel (1997)
Lake	Algal growth	Mathematical, process-based	Reynolds and Irish (1997)
Lake	Algal movement	Mathematical, process-based	Visser <i>et al.</i> (1997)

River	Algal growth and movement	Artificial Neural Networks	Whitehead <i>et al.</i> (1997)
River	Algal growth	Artificial Neural Networks	Wilson and Recknagel (1997)
River	Algal growth	Mathematical, process-based	Thebault and Qotbi (1998)
Lake	Algal growth	Mathematical, process-based	Frisk <i>et al.</i> (1999)
Lake	Algal growth	Mathematical, process-based	Kristov <i>et al.</i> (1999)
Lake	Algal movement	Mathematical, process-based	Wallace and Hamilton (2000)
River	Phytoplankton dynamics	Mathematical, process-based	Jeong <i>et al.</i> (2003)
River	Algal growth and movement	Mathematical, process-based	Guyen and Howard (2006b)
Lake	Algal growth movement	Mathematical, process-based	Hiroshi <i>et al.</i> (2008)
Lake	Population dynamics	Mathematical, process-based	Jöhnk <i>et al.</i> (2010)

Yet, the best approach that should be undertaken for the management of algal blooms is the prevention of bloom formation. This can be achieved by controlling the factors, which favour the growth of algae including nutrient and light.

Ömerli Reservoir is mainly affected by domestic and industrial wastewater discharge (Albay & Akçaalan, 2003). As a result, eutrophication and algal blooms have occurred as a great concern in the reservoir, frequently. For example, lately, thousands of fish (mainly *Cyprinus Carpiot L.*, 1758) died from high level of algal toxins (microcystin) (Albay and Akçaalan, 2003). The objective of this study to provide predictions about the intensity, timing, and location of potential algal blooms in three selected rivers of the Ömerli Reservoir. Therefore, in scope this study, a deterministic-mathematical algal growth and transport model (Guyen and Howard, 2006b) is applied to the streams of Ömerli Reservoir. The model consists of two sub-models including the growth rate and the movement components, which will be discussed further in the following chapter.

### 3. METHODOLOGY

#### 3.1. Site Description

Ömerli Reservoir is of great importance with its 23.1km<sup>2</sup> surface area, 100 km coast line, 220 milion m<sup>3</sup> water capture capacity, and 621 km<sup>2</sup> protection area. Ömerli Reservoir was established in 1972, to provide potable water for the city of İstanbul. It provides 48% of daily drinking water supply (872000m<sup>3</sup>) of the city and is the biggest reservoir in northern part of the Marmara Region.

The Riva Stream arises from Ömerli Reservoir border, flows North and Northwest in a rural grassland and discharges its waters into the Black Sea near the Riva Village. It is approximately 33 km in length. The main tributaries contributing to the Riva Stream are Alibahadır Stream, Kanlı Stream, and Karanlık Stream. The catchment area covers approximately 251 km<sup>2</sup> with 17616 inhabitants. The majority of the basin is covered by forests 76%. Approximately, 20% of the basin consists of agricultural land, fields and meadows (Temel, 2006). There are several animal husbandry farms in the agricultural land areas along the river banks (Dinseven and Çurgunlu, 1988). Paşaköy stream is surrounded by residential and business areas. Kömürlük Creek is often covered with trees. Kömürlük Stream water is used for irrigation of agricultural land of the near villages and it discharges its water into the Ömerli Reservoir (Tarkan, 2007). A schematic illustration of Riva, Paşaköy, and Kömürlük Rivers in the Ömerli Reservoir, and the topographical map of the catchment area together with water quality sampling stations are provided in Figures 3.1 and 3.2, respectively.

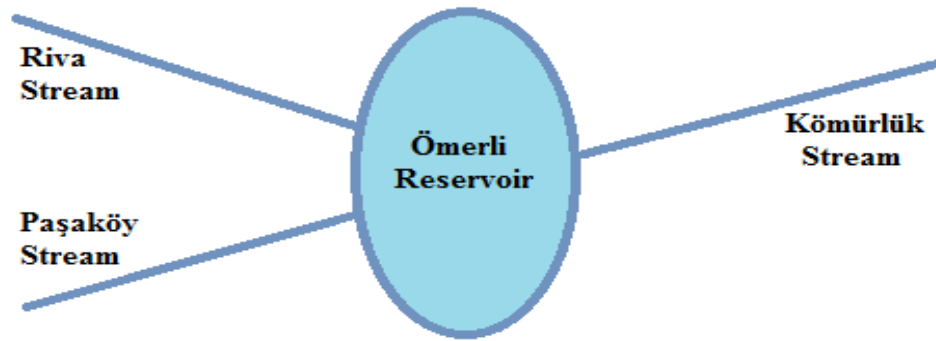


Figure 3.1. Illustration of Riva, Paşaköy, and Kömürlük Rivers in the Ömerli Reservoir.



Figure 3.2. The topographical map of the Ömerli Reservoir catchment area and the sampling stations of rivers. (Source:  $41^{\circ} 31' 07.84''$  N and  $29^{\circ} 22' 38.57''$  E. Google Earth. October 04, 2013).

### 3.2. Model Description

A formerly developed algal growth and movement model (Güven and Howard, 2006b) is applied to the streams of Ömerli Reservoir. The model consists of two sub-models: The growth rate and the movement sub-models.

For modeling the growth of algae, Michaelis–Menten type empirical equations are used to estimate the light, nutrient, and temperature dependencies of algal growth to determine the sinking velocities of the colonies:

$$\frac{d\rho}{dt} = \left( c_1 \left( \frac{\bar{I}_z}{K_1 + \bar{I}_z} \right) - c_2 I_a - c_3 \right) \min \left( \frac{N}{K_N + N}, \frac{P}{K_P + P} \right) \theta^{(T-20)} \quad (3.1)$$

where  $d\rho/dt$  is the change in density with time ( $\text{kg m}^{-3} \text{min}^{-1}$ ),  $c_1$  the rate coefficient determining the increase in density with time ( $\text{kg m}^{-3} \text{min}^{-1}$ ),  $c_2$  is the light-dependent rate coefficient describing the decrease in density with time ( $\text{kg m}^{-3} \text{min}^{-1}$ ),  $c_3$  is the minimal rate of density decrease ( $\text{kg m}^{-3} \text{min}^{-1}$ ),  $\bar{I}_z$  is the average irradiance ( $\mu\text{mol m}^{-2} \text{s}^{-1}$ ), where  $I_a$  is the previous irradiance ( $\mu\text{mol m}^{-2} \text{s}^{-1}$ ),  $K_1$  is the irradiance at which the rate of density increase with time is half the maximal rate ( $25 \mu\text{mol m}^{-2} \text{s}^{-1}$ ), N (Nitrogen) and P (Phosphorus) are the concentrations,  $K_N$  and  $K_P$  are the half saturation constants for N and P, respectively.  $\theta$  is the temperature-activity coefficient. The resulting density change from the above equation is used to calculate the new colony density ( $\rho_2$ ):

$$\rho_2 = \rho_1 + P \frac{d\rho}{dt} \quad (3.2)$$

where  $\rho_1$  is the initial density of the colony ( $\text{kg m}^{-3}$ ),  $P$  is the time step (min) and  $(d\rho/dt)$  is the rate of density change ( $\text{kg m}^{-3} \text{min}^{-1}$ ).

The new density value calculated from Equation 3.2 can then be inserted into the Stoke's Formula to determine the sinking velocities of algal colonies:

$$v = 2gr^2(\rho_c - \rho')A/(9\phi n) \quad (3.3)$$

where  $g$  is the gravitational acceleration ( $9.81 \text{ m s}^{-2}$ ),  $r$  is the effective radius of the colony (m),  $\rho_c$  and  $\rho'$  are the densities of the cyanobacterium and water, respectively,  $A$  is the proportion of cell volume relative to colony volume,  $\phi$  the form resistance and  $n$  the viscosity of the water ( $\text{kg m}^{-1} \text{ s}^{-1}$ ).

During the modeling of algal transport, streamflow conditions are handled separately for laminar and turbulent flowing streams to reduce the number of parameters needed under laminar flow conditions, and to reflect the reality of turbulence in natural river channels, respectively. For laminar flows, the model combines the vertical velocity obtained from Equation 3.3 with the mean river velocity derived from Manning's equation:

$$u = \frac{C_0}{n_{roughness}} R^{2/3} S_e^{1/2} \quad (3.4)$$

where ( $u$ ) is mean river velocity,  $C_0$  is a constant,  $n_{roughness}$  is Manning's roughness coefficient (0.0030 for clean and straight, 0.0040 for clean and winding stream channels) (Chapra, 1997),  $R$  is channel's hydraulic radius (m), and  $S_e$  is the slope of the channel's energy grade line.

On the other hand, under the existence of turbulence, vertical sinking velocity is combined with the equation to account for the rivers' logarithmic velocity distribution:

$$u(z) = u^* \frac{1}{\kappa} \ln\left(\frac{d-z}{z_0}\right) \quad (3.5)$$

where  $u(z)$  is the velocity profile,  $u^*$  is the shear velocity,  $\kappa$  is von Karman's universal constant,  $d$  is the river depth,  $z$  is the distance from the water surface and  $z_0$  is the height where velocity is zero. According to Prandtl's mixing theory, velocity fluctuations in turbulent environments can be approximated as:

$$|u'| \approx |w'| \approx l \frac{d\bar{u}}{dz} \quad (3.6)$$

where  $|u'|$  and  $|w'|$  are the absolute values of the instantaneous lateral and vertical turbulent velocity fluctuations in time  $dt$ , respectively,  $l$  is a characteristic length known as the mixing length and  $du/dz$  is the velocity gradient.

For the determination of algal concentrations in stream reaches, mass balance equations are applied, and tanks – in – series approach is used, especially, to overcome the difficulties encountered in modeling the highly variable nature of river systems. Thus, mass-balance equations of the Continuously Stirred Tank Reactors (CSTR) are applied for each pre-determined reach of the river:

$$\frac{da}{dt} = \left[ k_{g,\max} \left( \frac{\bar{I}_z}{K_1 + \bar{I}_z} \right) \min \left( \frac{N}{K_N + N}, \frac{P}{K_P + P} \right) \theta^{(T-20)} - k_d \right] a + \frac{Q(a_{in} - a)}{V} \quad (3.7)$$

where  $a$  is the algal biomass concentration and is directly proportional to the concentration of chlorophyll- $a$  ( $\text{mg l}^{-1}$ ),  $Q$  is the flow ( $\text{l s}^{-1}$ ),  $V$  is the control volume and  $k_d$  is the death rate due to the combined effects of respiration and excretion. Typical values of  $k_d$  range between  $0.1$  to  $0.2 \text{ d}^{-1}$  and a  $\theta$  model is usually used to adjust the respiration or excretion rate according to the temperature (Chapra, 1997).

When supported by a computer simulation programme, CSTR application allows the user to set different values for the variables, parameters and constants for each reach of the river. Model equations that are used for this study are utilized by a computer simulation program (Güven and Howard, 2006b). The program allows the user to set the values of parameters, variables and monthly data for different segments of the river. An example of the screenshot of the computer simulation program showing the ‘Edit Parameters’ menu is provided in Figure 3.3.

Parameter	Value	Parameter	Value
Initial colony depth (m)	1.	Water density (kg/m <sup>3</sup> )	1000.
Initial colony density (kg/m <sup>3</sup> )	980.	Hydraulic radius (m)	1.
Day length (min)	600.	Slope of energy gradline	0.005.
Ammonium (mg/m <sup>3</sup> )	0.	River depth (m)	4.
Nitrite concentration (mg/m <sup>3</sup> )	0.	Surface slope	0.005.
Nitrate concentration (mg/m <sup>3</sup> )	500.	Flow (m <sup>3</sup> /s)	10.
Phosphate concentration (mg/m <sup>3</sup> )	20.	Pre. ave. irradiance (μmol/(m <sup>2</sup> s))	38.
Initial biomass (mg/m <sup>3</sup> )	9.	External Nitrogen load (mg/m <sup>3</sup> )	20.
Cell volume / Colony volume	1.	External Phosphorus load (mg/m <sup>3</sup> )	20.
Form resistance	1.		
Colony radius (μm)	200.		

Figure 3.3. A screenshot of the computer simulation program showing the 'Edit Parameters' menu.

Accordingly, to be able to set the model and for subsequent model validation steps, topographical and water quality data are used as the input data in order to determine the algal concentrations in selected streams of the Ömerli Reservoir. The data and information flowchart is illustrated in Figure 3.4.

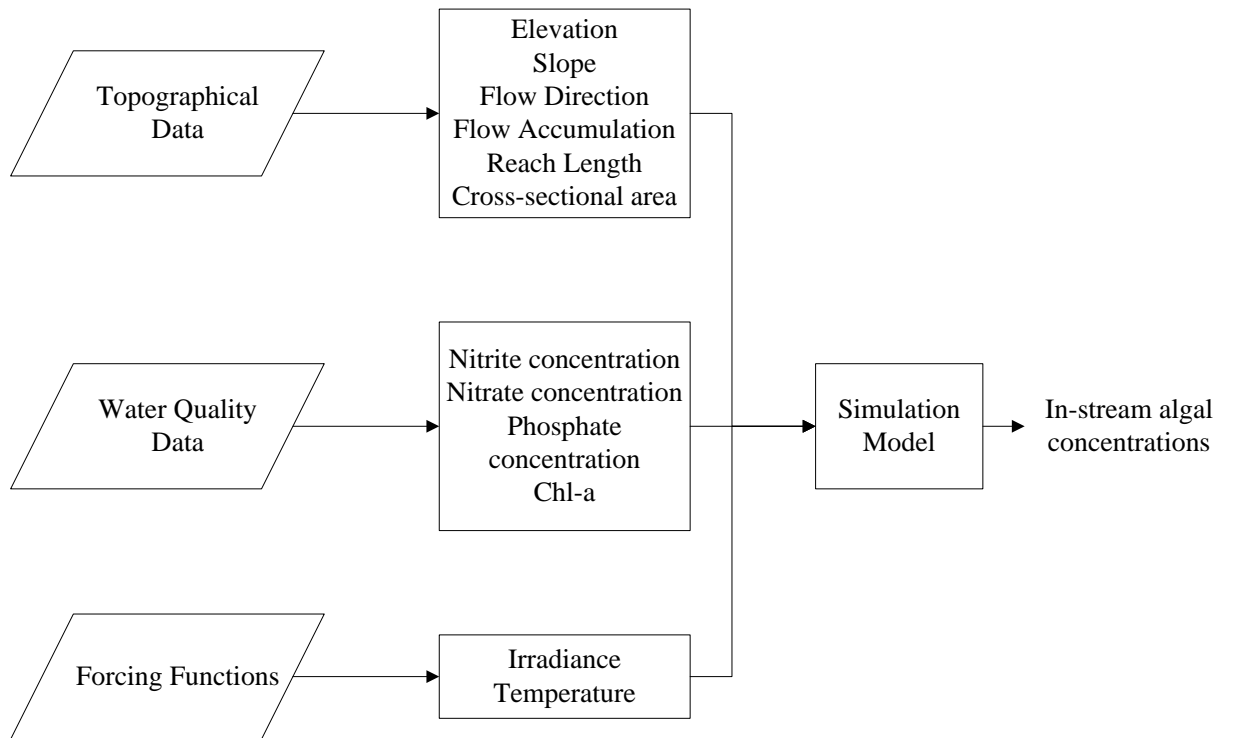


Figure 3.4. A schematic representation of information flow.

### 3.3. Data Requirements

The main variables regarding the model, which were briefly described in the previous section, can be classified as forcing functions and state variables as given in Table 3.1.

Table 3.1. The model variables.

<b>Forcing functions</b>	<b>State variables</b>
Solar irradiance (I)	Algae density ( $\rho$ )
Daylength period (DL)	Algae concentration (X)
Temperature (T)	Algae growth rate (dp/dt)
Nitrogen (additions to flow)	Settling velocity (v)
Phosphorus (additions to flow)	Nitrogen (internal transformations)
Mean river flow (Q)	Phosphorus (internal transformations)
Mean river velocity (U)	
Riverbed shear stress ( $\tau_0$ )	
Volume of tank (V)	

Data requirements for any modeling work generally fall under two main categories: (i) Calibration data, which are required to set initial parameter values, and, (ii) validation data, to be used to check whether the model produces reasonable outcomes. Since the model that is used in this study is a formerly developed and calibrated model, all the data obtained and summarized in this section are used for model set up and validation purposes, only. Model is set up for the Riva River, by using water quality data from Temel (2006) and Tarkan (2007), and model validation is carried out mostly for Paşaköy and Kömürlük Rivers, with the data obtained from Tarkan (2007).

As with most water quality models that are developed for rivers, the initial step is to divide the river system into reaches, which are the stretches of the river having approximately uniform characteristics. For this purpose, the study area as illustrated in Figure 3.1., is topographically analyzed by using Geographical Information Systems (GIS), to determine the direction of flow within the catchment area, the individual reach distances and slopes of the streams in the reservoir.

### **3.3.1. Topographical Data**

The accurate derivation of system's topographical characteristics plays an important role in modeling fluvial systems. Topographic data such as slope, elevation, and flow characteristics, which are the most crucial catchment characteristics, are determined by the use of ArcGIS 10 software. In addition, the distances between the sampling stations are derived. Furthermore, to be able to visualize the catchment clearly, flow direction and accumulation maps are derived.

The initial step in the determination of these maps are the preparation of elevation and associated slope parameters. To achieve this, first of all, a digital elevation map layer is added to the ArcGIS software as backdrop to create digital elevation model (DEM) and to produce maps with the required topographical information. Surface elevation is the key in determining most of the GIS based maps, such as slope, flow direction and flow accumulation. Because every pixel of the digital elevation map includes elevation and coordinate information, it is used as a base map. Using the spatial analyst tool of ArcGIS, maps regarding gradual elevation and slope are produced. The direction of river flow can be determined by the "Flow Direction" function of the ArcGIS for every cell in the grid by using elevation and slope information. Although the direction of flow information was already obvious, this function also acts as a preceding step for accessing flow accumulation information, which is derived to be able to provide a more clear GIS-based representation of the study area map.

Gradual elevation, slope, flow direction and flow accumulation maps of the study area are provided in Figures 3.5., 3.6., 3.7. and 3.8., respectively.

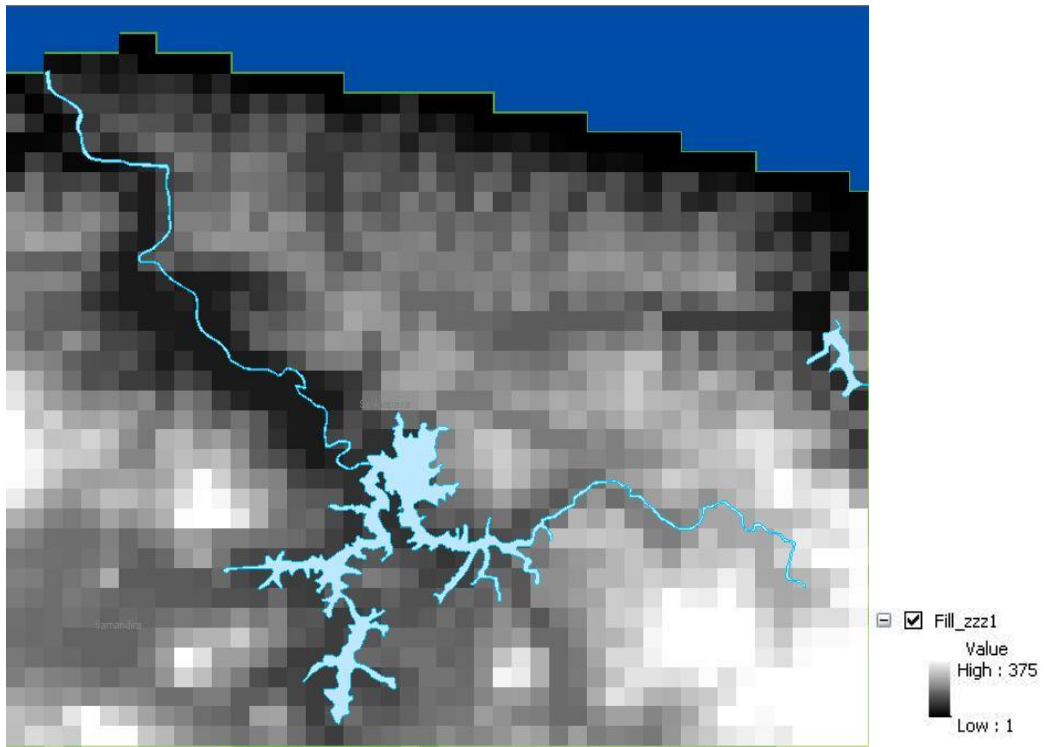


Figure 3.5. Elevation map of the Ömerli Reservoir.

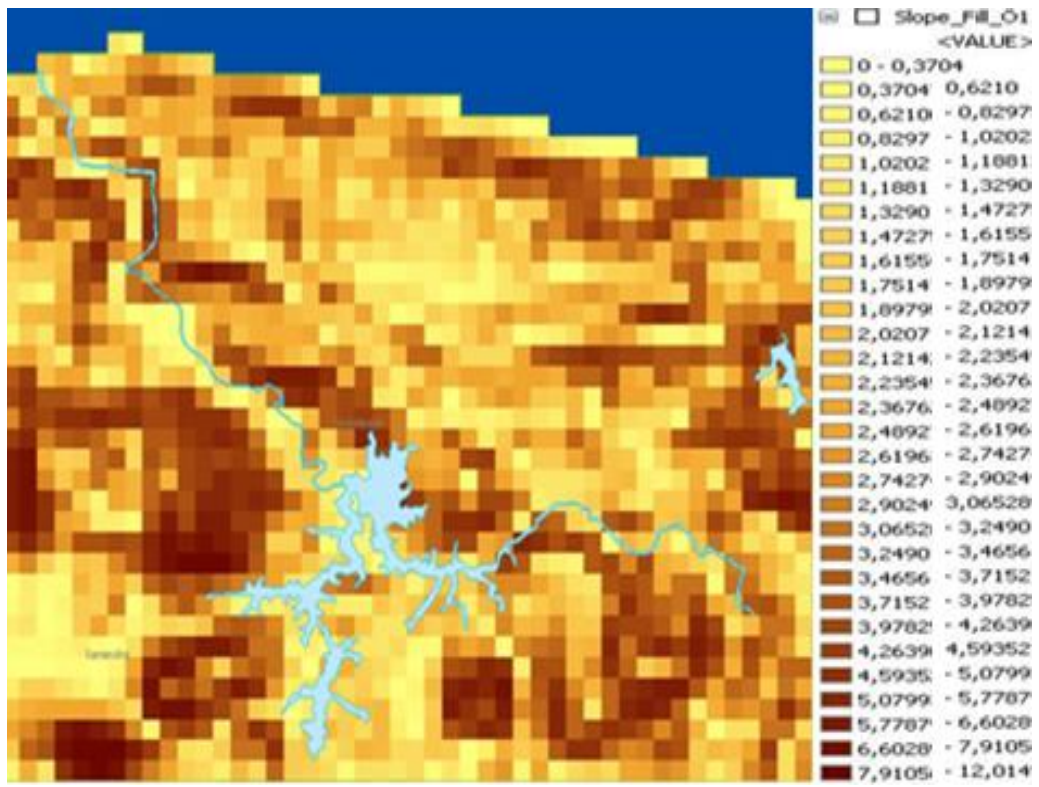


Figure 3.6. Slope map of the Ömerli Reservoir.

The output of flow direction is an integer raster whose values range from 1 to 128 and each color in the map corresponds to such a value in that range. The values for each direction from the center are given in Figure 3.7.

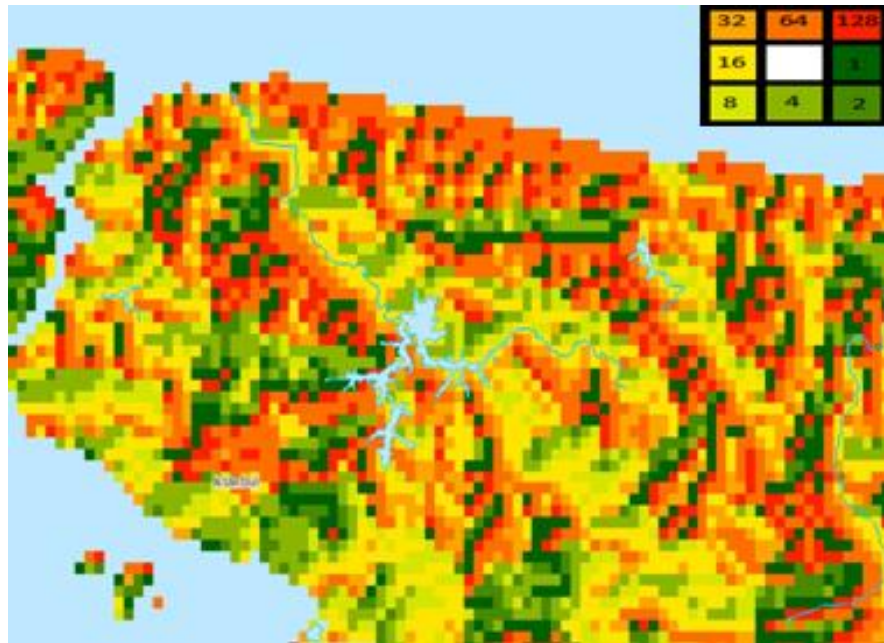


Figure 3.7. Flow direction map of the Ömerli Reservoir.



Figure 3.8. Flow accumulation of the Ömerli Reservoir.

### 3.3.2. River Quality Data

Model is set up for the Riva River, by using water quality data from Temel (2006) and Tarkan (2007), and the validation step is done for Paşaköy and Kömürlük Rivers, by the data obtained from Tarkan (2007). Table 3.2 summarizes the type of data and their sources for 13 river stations around the Ömerli Reservoir. The characteristics of the data used in the model application are provided in Tables 3.3 to 3.6.

Table 3.2. Summary of the river quality data that is used in the model.

Station number	Data	Source
Riva River A	Water quality (Table 3.3)	Temel (2006)
Riva River B	Water quality (Table 3.3)	Temel (2006)
Riva River C	Water quality (Table 3.3)	Temel (2006)
Riva River D	Water quality (Table 3.3)	Temel (2006)
Riva River E	Water quality (Table 3.3)	Temel (2006)
Riva River F	Water quality (Table 3.3)	Temel (2006)
Riva River G	Water quality (Table 3.3)	Temel (2006)
Riva River 1	Water quality, Chl- <i>a</i> (Table 3.4)	Tarkan (2007)
Riva River 2	Water quality, Chl- <i>a</i> (Table 3.4)	Tarkan (2007)
Paşaköy River 1	Water quality, Chl- <i>a</i> (Table 3.5)	Tarkan (2007)
Paşaköy River 2	Water quality, Chl- <i>a</i> (Table 3.5)	Tarkan (2007)
Kömürlük River 1	Water quality, Chl- <i>a</i> (Table 3.6)	Tarkan (2007)
Kömürlük River 2	Water quality, Chl- <i>a</i> (Table 3.6)	Tarkan (2007)

Table 3.3. Physical, chemical and biological data of the Riva River.

Parameters	A	B	C	D	E	F	G
Temperature ( $^{\circ}\text{C}$ )	available *	available *	available *	available *	available *	available *	available *
DO ( $\text{mg L}^{-1}$ )	available *						
Nitrate ( $\text{mg L}^{-1}$ )	available *	available *	available *	available *	available *	available *	available *
Nitrite ( $\text{mg L}^{-1}$ )	available *	available *	available *	available *	available *	available *	available *
Phosphate ( $\text{mg L}^{-1}$ )	available *	available *	available *	available *	available *	available *	available *
Turbidity (420nm)	available *	available *	available *	available *	available *	available *	available *
pH	available *	available *	available *	available *	available *	available *	available *
Total hardness	available *	available *	available *	available *	available *	available *	available *
Salinity (%)	available *						
Algal abundance	available *	available *	available *	available *	available *	available *	available *

\*Monthly water samples were collected from 7 stations in the Riva Stream between August, 2002 and August, 2003 (Temel, 2006).

Table 3.4. Physical, chemical and biological characteristics of the Riva River data.

Data Type	Station-1 Data	Station-2 Data
Temperature ( $^{\circ}\text{C}$ )	1 year monthly data available except for Jan 06*	1 year monthly*
Light (lux)	1 year monthly data available except for Jan 06*	1 year monthly*
Depth (cm)	1 year monthly data available except for Jan 06*	-
Width (cm)	1 year monthly data available except for Jan 06*	-
Flow ( $\text{ms}^{-1}$ )	1 year monthly data available except for Jan 06*	-
TDS ( $\text{mg L}^{-1}$ )	1 year monthly data available except for Jan 06*	1 year monthly*
SSP ( $\text{mg L}^{-1}$ )	1 year monthly data available except for Jan 06*	1 year monthly*
DO ( $\text{mg L}^{-1}$ )	1 year monthly data available except for Jan 06*	1 year monthly*
o- $\text{PO}_4$ ( $\mu\text{g L}^{-1}$ )	1 year monthly*	1 year monthly data available except for Jan 06* and Oct 05*
TP ( $\mu\text{g L}^{-1}$ )	1 year monthly data available except for Aug 05*	1 year monthly data available except for Jan 06* and Aug 05*
$\text{SO}_4$ ( $\text{mg L}^{-1}$ )	1 year monthly*	1 year monthly data available except for Jan 06*
$\text{NO}_2\text{-N}$ ( $\mu\text{g L}^{-1}$ )	1 year monthly*	1 year monthly data available except for Jan 06*
$\text{NO}_3\text{-N}$ ( $\text{mg L}^{-1}$ )	1 year monthly*	1 year monthly data available except for Jan 06*
$\text{SiO}_2$ $\mu\text{g L}^{-1}$	1 year monthly*	1 year monthly data available except for Jan 06*
Salinity	1 year monthly*	1 year monthly data available except for Jan 06*
Fe	1 year monthly*	1 year monthly data available except for Jan 06*
pH	1 year monthly data available except for Jan 06*	1 year monthly*
Chl- <i>a</i> ( $\mu\text{g/l}$ )	1 year monthly data available except for Jan 06*	1 year monthly*

\* Data were collected from 2 stations of the Riva stream monthly between 06/ 2005 - 07/ 2006 (Tarkan, 2007).

Table 3.5. Physical, chemical and biological characteristics of the Paşaköy River data.

Data Type	Station -1 Data	Station-2 Data
Temperature ( $^{\circ}\text{C}$ )	1 year monthly*	1 year monthly data available except for Jan 06*
Light (lux)	1 year monthly*	1 year monthly data available except for Jan 06*
Depth (cm)	1 year monthly*	-
Width (cm)	1 year monthly*	-
Flow ( $\text{ms}^{-1}$ )	1 year monthly*	-
TDS ( $\text{mg L}^{-1}$ )	1 year monthly*	1 year monthly data available except for Jan 06*
SSP ( $\text{mg L}^{-1}$ )	1 year monthly*	1 year monthly data available except for Jan 06*
DO ( $\text{mg L}^{-1}$ )	1 year monthly data available except for Jan 06*	1 year monthly data available except for Jan 06*
o-PO4 ( $\mu\text{g L}^{-1}$ )	1 year monthly*	1 year monthly data available except for Jan 06*
TP ( $\mu\text{g L}^{-1}$ )	1 year monthly data available except for Aug 05*	1 year monthly data available except for Jan 06*
SO <sub>4</sub> ( $\text{mg L}^{-1}$ )	1 year monthly*	1 year monthly data available except for Jan 06*
NO <sub>2</sub> -N ( $\mu\text{g L}^{-1}$ )	1 year monthly*	1 year monthly data available except for Jan 06*
NO <sub>3</sub> -N ( $\text{mg L}^{-1}$ )	1 year monthly*	1 year monthly data available except for Jan 06*
SiO <sub>2</sub> $\mu\text{g L}^{-1}$	1 year monthly*	1 year monthly data available except for Jan 06*
Salinity	1 year monthly*	1 year monthly data available except for Jan 06*
Fe	1 year monthly*	1 year monthly data available except for Jan 06*
pH	1 year monthly*	1 year monthly data available except for Jan 06*
Conductivity ( $\mu\text{S cm}^{-1}$ )	1 year monthly*	1 year monthly data available except for Jan 06*
Chl- <i>a</i> ( $\mu\text{g/l}$ )	1 year monthly*	1 year monthly data available except for Jan 06*

\*Data were collected from 2 sampling stations of the Paşaköy River monthly between 06/ 2005-07/ 2006 (Tarkan, 2007).

Table 3.6. Physical, chemical and biological characteristics of the K m rl k River Data.

Data Type	Station -1 Data	Station-2 Data
Temperature ( $^{\circ}\text{C}$ )	1 year monthly*	1 year monthly data available except for Jan 06*
Light (lux)	1 year monthly*	1 year monthly*
Depth (cm)	1 year monthly*	-
Width (cm)	1 year monthly*	-
Flow ( $\text{m s}^{-1}$ )	1 year monthly*	-
TDS ( $\text{mg L}^{-1}$ )	1 year monthly*	1 year monthly*
SSP ( $\text{mg L}^{-1}$ )	1 year monthly*	1 year monthly*
DO ( $\text{mg L}^{-1}$ )	1 year monthly*	1 year monthly*
o-PO4 ( $\mu\text{g L}^{-1}$ )	1 year monthly*	1 year monthly*
TP ( $\mu\text{g L}^{-1}$ )	1 year monthly*	1 year monthly*
SO <sub>4</sub> ( $\text{mg L}^{-1}$ )	1 year monthly*	1 year monthly*
NO <sub>2</sub> -N ( $\mu\text{g L}^{-1}$ )	1 year monthly*	1 year monthly*
NO <sub>3</sub> -N ( $\text{mg L}^{-1}$ )	1 year monthly*	1 year monthly*
SiO <sub>2</sub> ( $\mu\text{g L}^{-1}$ )	1 year monthly*	1 year monthly*
Salinity	1 year monthly*	1 year monthly*
Fe	1 year monthly*	1 year monthly*
pH	1 year monthly*	1 year monthly*
Conductivity ( $\mu\text{S cm}^{-1}$ )	1 year monthly*	1 year monthly*
Chl- <i>a</i> ( $\mu\text{g/l}$ )	1 year monthly*	1 year monthly*

\*Water samples were collected from 2 sampling stations of the K m rl k River monthly between June, 2005 and July, 2006. (Tarkan, 2007).

## 4. RESULTS AND DISCUSSIONS

Despite the fact that the model was calibrated (Güven and Howard, 2006b) and qualitatively validated before (Güven and Howard, 2007), in this study, real field data including both topographical and river quality characteristics, were applied to the model. Therefore, first of all, it is necessary to carry out a verification of the model to observe whether the simulations produced with data carrying different characteristics illustrates reasonable outcomes. By using the model algorithms in the model described in Chapter 3, a number of simulations are produced to compare the outputs produced with real field values with the results produced by using previously calibrated values. The results of the model verification are given in section 4.1.

Secondly, a number of simulation results are produced based on the data given in Tables between 3.2 and 3.6. The simulations are chosen to account for the changes in major environmental variables, such as light, temperature, nutrients, to observe the effects on algal growth and transport. Section 4.2 discusses the effects of changes in major environmental variables on algal density and colony growth, and section 4.3 describes the effects of those on the colony movement.

### 4.1. Verification of the Model

It is important that the verification step is carried out for all three rivers modeled in the scope of this study. Therefore, colony density and depth simulations are undertaken for the K m rl k, Pařak y, and Riva Streams. An example of dataset and corresponding sources used in the model are outlined in Table 4.1, for the K m rl k River. Figures from 4.1 to 4.6 have a responsive agreement between simulated and previously calibrated values. As the simulation result suggests reasonable trend between the calibrated and simulated values in density and depth curves, it can be concluded that model application can provide a good representation of movement and growth of algae.

Table 4.1. Data of the K m rl k River is used in the model.

<b>Data Type</b>	<b>Units</b>	<b>Source</b>
Nitrite concentration	mg m <sup>-3</sup>	(Temel, 2006; Tarkan, 2007)
Nitrate concentration	mg m <sup>-3</sup>	(Temel, 2006; Tarkan, 2007)
Phosphate concentration	mg m <sup>-3</sup>	(Temel, 2006; Tarkan, 2007)
Chl- <i>a</i>	�g l <sup>-1</sup>	(Temel, 2006; Tarkan, 2007)
Temperature	�C	(Temel, 2006; Tarkan, 2007)
Irradiance	�mol m <sup>-2</sup> s <sup>-1</sup>	(Tarkan, 2007)
Surface slope	dimensionless	GIS based data system
River depth	m	(Tarkan, 2007)
River flow	m s <sup>-1</sup>	(Tarkan, 2007)
Reach length	m	GIS based data system
Cross-sectional area	m <sup>2</sup>	(Tarkan, 2007)

Carbohydrate is fixed in algal cells during photosynthetic activity, and the yield of photosynthetically fixed carbon is accumulated in algal cells in the form of glycogen (Reynolds *et al.*, 1987). Overall density of algae increases by increasing carbohydrate accumulation in the cells. As a consequence of decreasing photosynthetic activity at night, carbohydrate is consumed as a result of metabolic activity, causing a decrease in the overall density of the algae. This is called the cell balast mechanism (Reynolds *et al.*, 1987). As a result of this mechanism cellular buoyancy of algae is regulated. Thus, the growth of algal colonies follow an oscillatory pattern due to the diurnal changes in solar irradiance and density change as illustrated in Figures 4.1, 4.2 and 4.3, for the K m rl k, Pa ak y and Riva Rivers, respectively. As these figures indicate model calibration and simulation trends are in harmony with each other, the model seems to be capable of describing the algal behaviour with the data obtained from field studies.

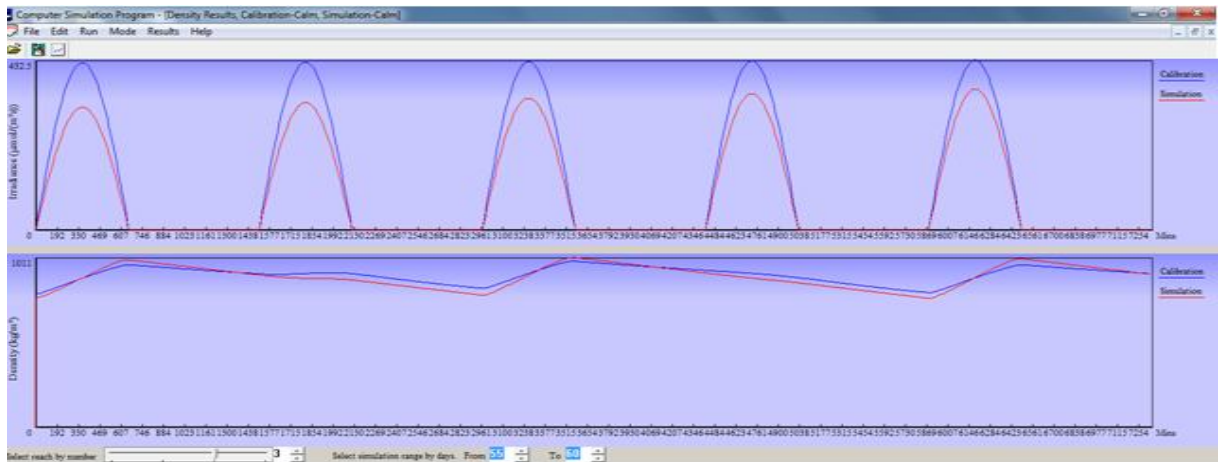


Figure 4.1. Simulation of colony density for the Kömürlük River: Reach 2.

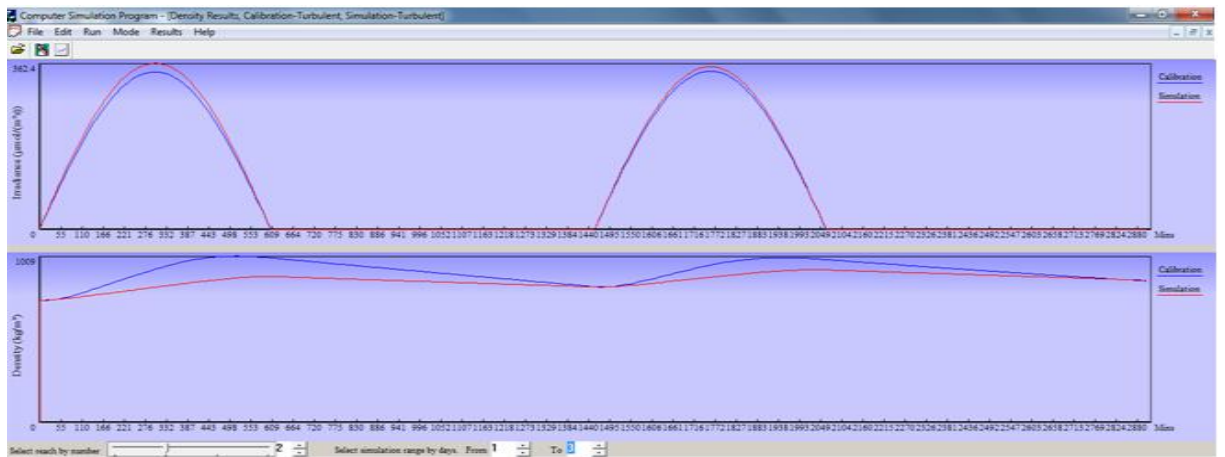


Figure 4.2. Simulation of colony density for the Paşaköy River: Reach 2.

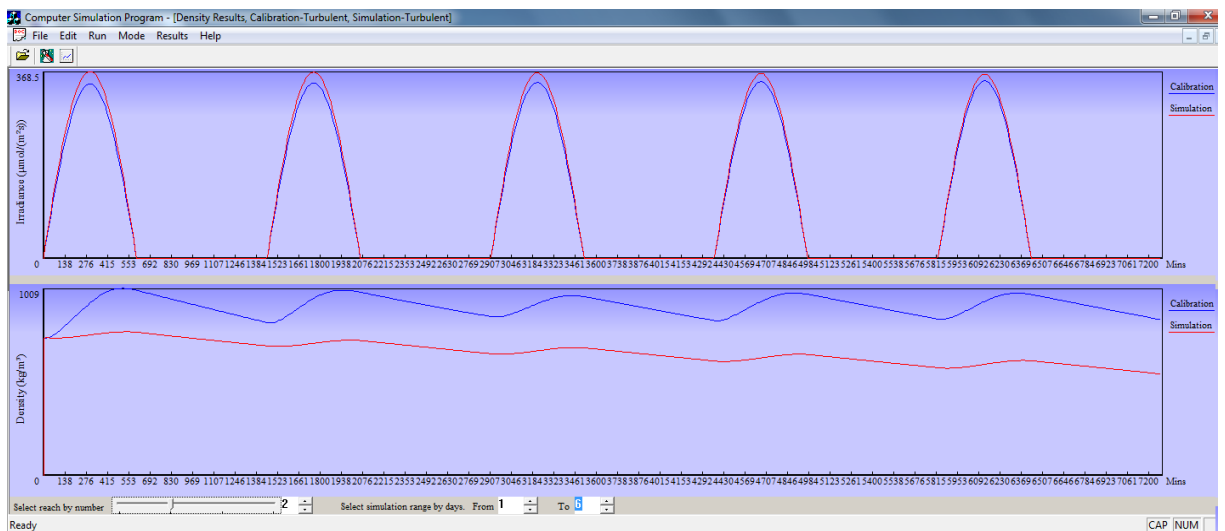


Figure 4.3. Simulation of colony density for the Riva River: Reach D and Reach C.

The rate of density change plays an important role in buoyancy regulation of algal cells, affecting both growth and movement of algal colonies. Similar to the growth of algae, movement of the colonies also behaves in a iterative manner, following an oscillatory pattern. This is mainly because, buoyancy of algae depends on the colony density in relation to the surrounding water density. This effect can clearly be seen in Figures 4.4., 4.5., and 4.6., for the K m rl k, Pařak y and Riva Rivers, respectively. For the simulations the river depth is taken as 4m (Temel, 1994). The vertical migration occurs until the colony density reaches the surrounding water density. As the cells begin to receive enough irradiance at the upper layers of the water column, carbohydrate accumulation occurs resulting in an increase in the overall density of algae and colony sinks. As the following figures suggest there is a good trend between the calibrated and simulated values in density and depth curves, therefore it can be concluded that model application can illustrate a reasonable representation of the movement of algae.

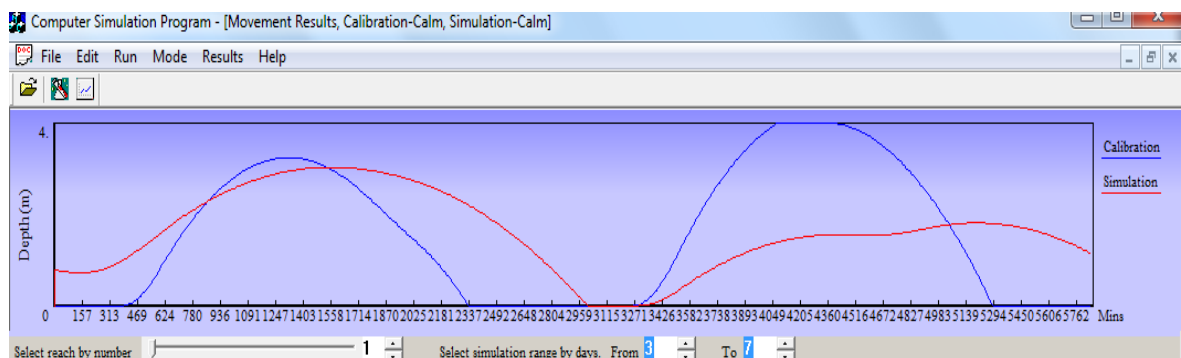


Figure 4.4. Simulation of colony depth for the K m rl k River: Reach2.

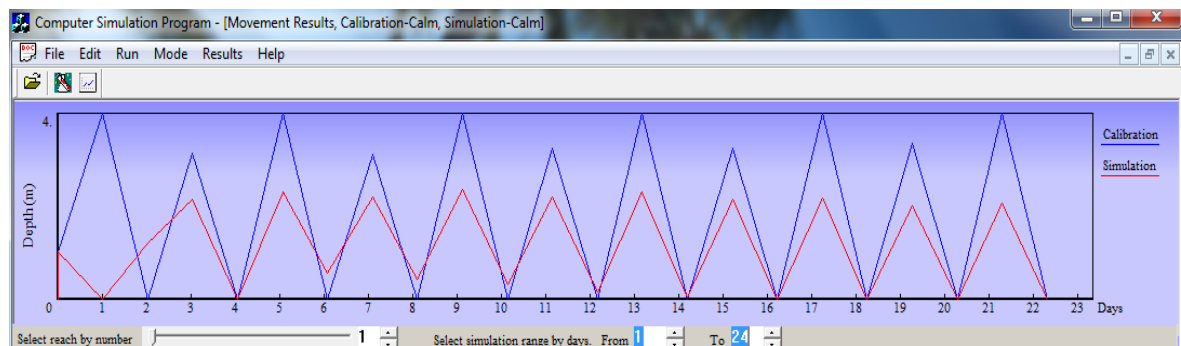


Figure 4.5. Simulation of colony depth for the Pařak y River: Reach 1.

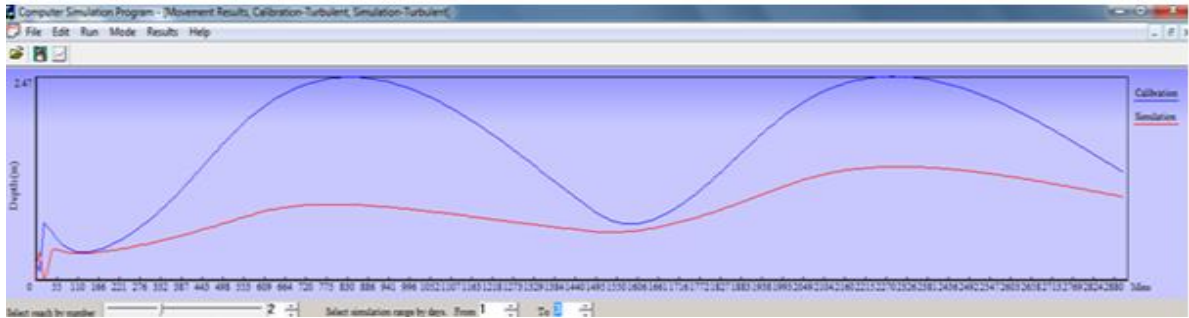


Figure 4.6. Simulation of colony depth for the Paşaköy River: Reach 2.

## 4.2. Results of the Growth Model

The literature about the metabolism and growth of algae is wide and mostly explained and reviewed by Fogg (1969), Fogg *et al.* (1973), and Reynolds and Walsby (1975). According to Kromkamp and Mur (1984), accumulation of carbohydrate ballast is the main mechanism in density regulation in *Microcystis* sp. and there is a linear relationship between the cell density and cell carbohydrate content. In this section increased carbohydrate content and cell density is referred to as algal growth. The key factors affecting the growth of algae in freshwaters consist of light, temperature, and chemical composition (Nitrite, Nitrate, Phosphate, and Ammonium) of the water column. Most importantly, irradiance has a critical importance on colony growth of algae.

### 4.2.1. Effect of Day Length on Colony Growth

The light intensity received by the colonies, is amongst the most significant factors that influences the buoyant state of the cyanobacteria, and it is affected by a number of factors including the length of the light period. In order to observe the effect of day length on the colony growth, the model is run for two different day length periods. In the calibration run, the day length is assumed to be 10 hours, and in the simulation it is increased to 16 hours. It has been generally acknowledged that density increase occurs as a result of carbohydrate deposition, and under continuous illumination the rate of density gain of algae is linear (*e.g.* Kromkamp and Walsby, 1990; Howard *et al.*, 1996; Visser *et al.*, 1997). More recently, Wallace and Hamilton (2000) suggested that the rate of increase in carbohydrate and cell density does not instantaneously adjust to an increase in light intensity. According to the authors there was a time lag, the response time, corresponding

to physiological adjustment to the increase in light, before the equilibration of the rate of carbohydrate and density increase. Figure 4.7 combines these two findings from previous studies, and is important for two aspects: First of all, the graph shows that the density gain happens under high solar intensities, from dawn to noon and a linear decline in density starts to occur in the dark. Secondly, while the irradiance begins to increase again after the first dark period, density still continues to decrease. This can be explained by the response time of algae to adjust its carbohydrate ballast to the changes in irradiance. According to Wallace and Hamilton (2000), this effect is predicted to be more significant when colonies are entrained in mixing. As Figure 4.7. suggests, simulation results agrees well with the findings in the literature.

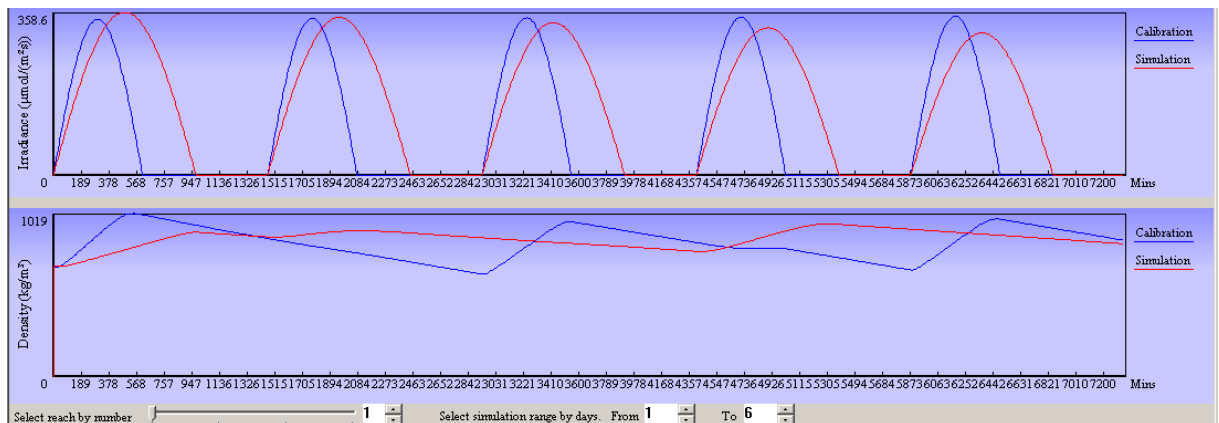


Figure 4.7. Simulation of colony density for the Riva River Reach 1.

#### 4.2.2. Effect of Irradiance on Colony Growth

Solar irradiance is a crucial resource for the photoautotrophy; thus, irradiance affects the richness of algae in freshwaters as a governing factor. Photosynthetic activity increases by rising irradiance intensity and the relation with photosynthesis and light intensity can be described by a Michaelis- Menten type equation (Zevenboom and Mur, 1984; Kromkamp and Walsby, 1990; Howard, 1993; Visser *et al.*, 1997). Figure 4.8 illustrates that the K m rl k River has a good correlation between chlorophyll-*a*, irradiance and density trends. As the photosynthesis starts to take place as result of increasing irradiance, carbohydrate begins to be produced and algal density increases. However, it is clear that there is a time lag between peak irradiance and density values, which is a result of the response time of algae to accumulate carbohydrate ballast as reported by Wallace and

Hamilton (1999). The simulation given in Figure 4.8 includes the period between the end of February to mid-July. According to the figure, chlorophyll-*a* concentrations begin to increase in May, making a peak in the beginning of June, and then starts to decrease until it approximates to the normal seasonal Chl-*a* levels. According to the results of the model algal blooms in the K m rl k River are most likely to occur between late spring and mid summer. This situation can also be related the water temperatures, as the optimum water temperature for most of the bloom-forming species ranges between 25-35 C (Fogg et al., 1973, Reynolds and Walsby, 1975;). This relation between the irradiance and colony density can also be observed in Figure 4.9., for the Pa ak y River.

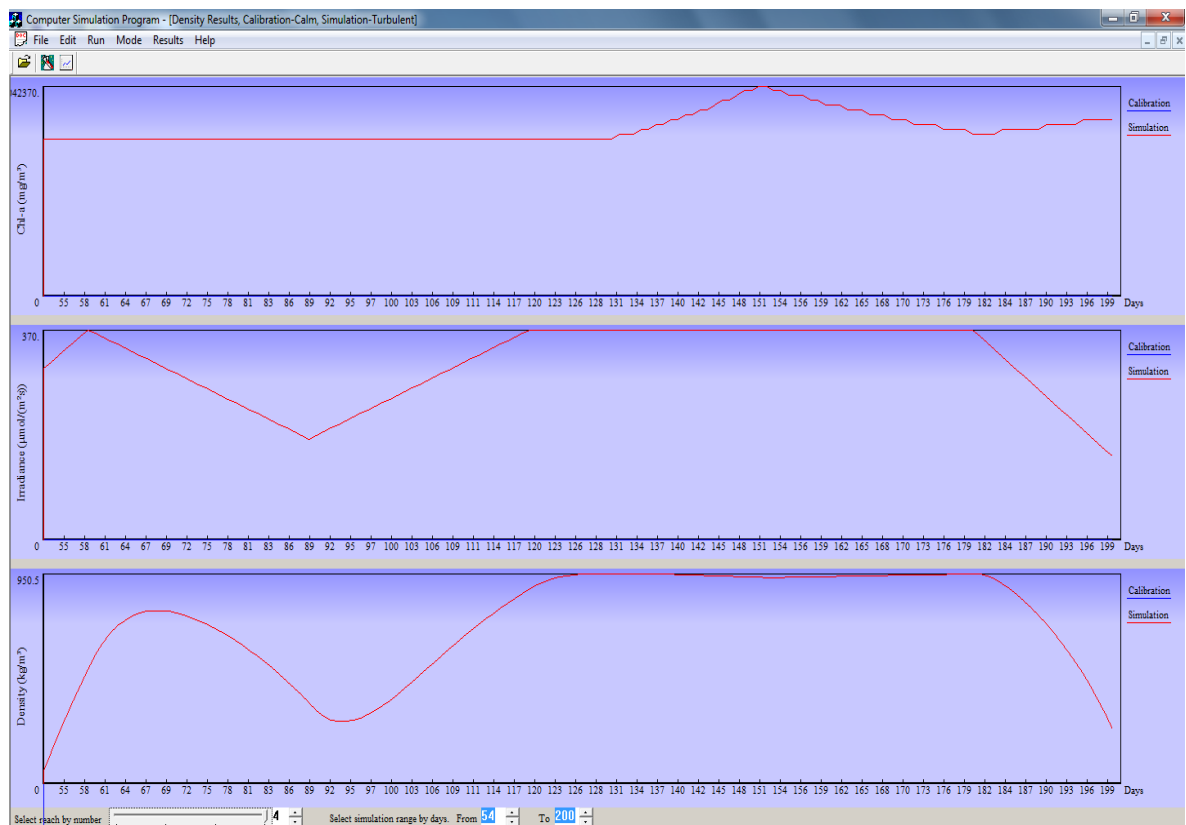


Figure 4.8. Simulation of colony density for the K m rl k River: Reach 2.

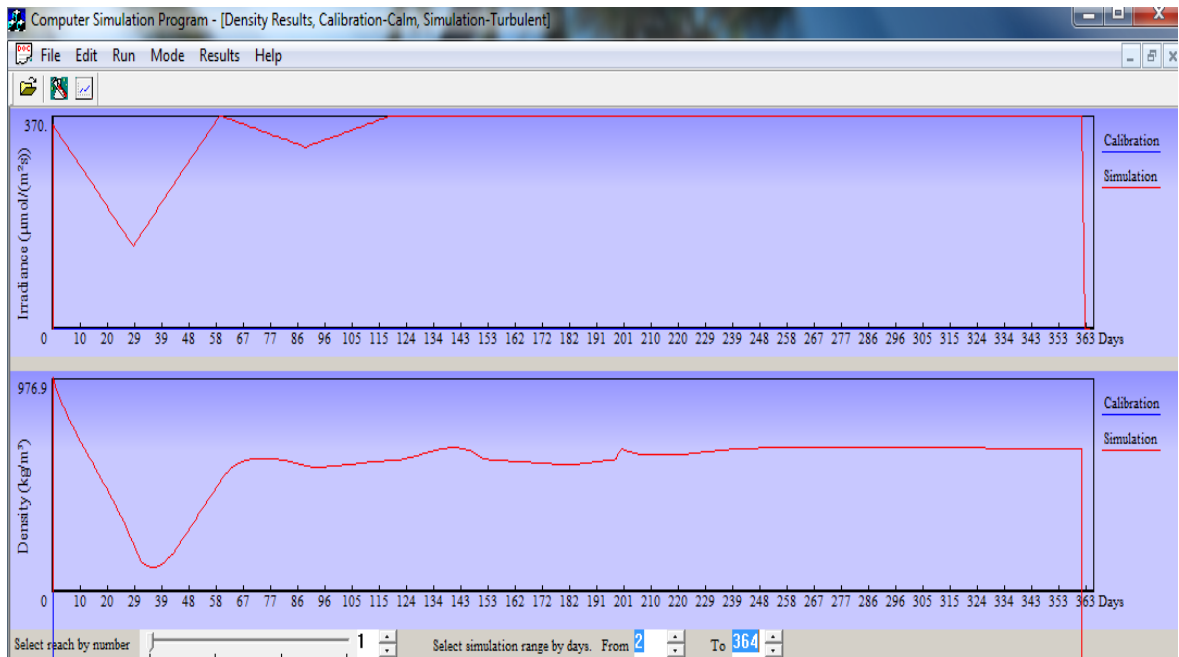


Figure 4.9. Simulation of colony density for the Paşaköy River: Reach 1.

Figures 4.10 and 4.11 illustrates the seasonal variations in algal density over a year period for the different reaches of the Riva River. According to the model, although there is a chance of algal bloom for a relatively short period of time in the beginning of March, surface blooms and associated eutrophication problem seems more persistent between late April and early August for the Riva River.

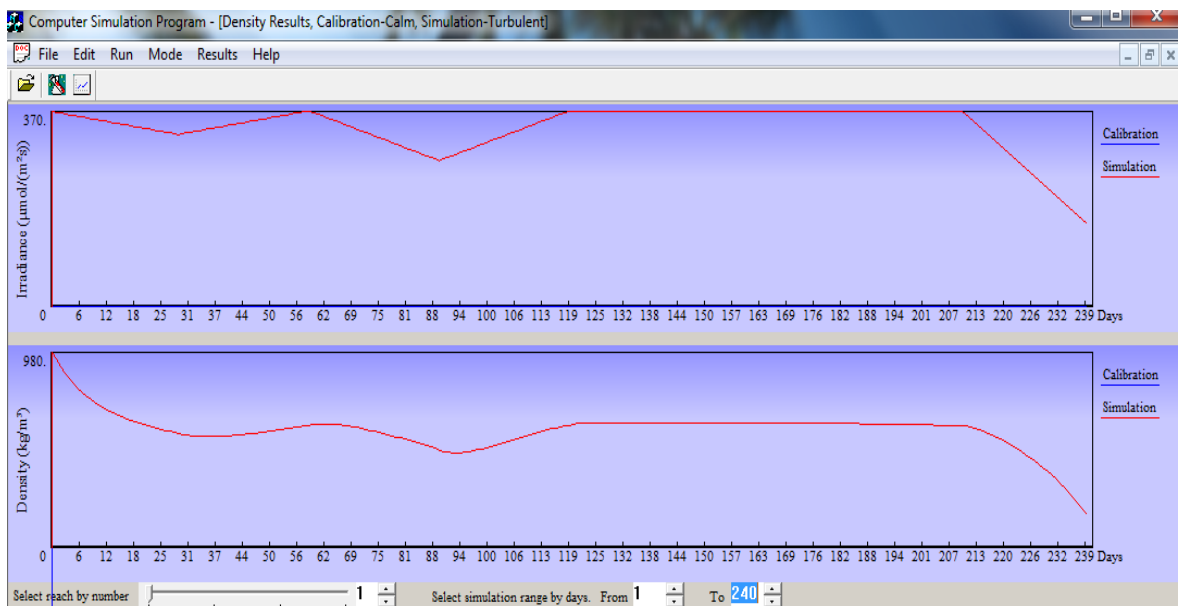


Figure 4.10. Simulation of colony density for the Riva River: Reach 1,2,G, F, and E.

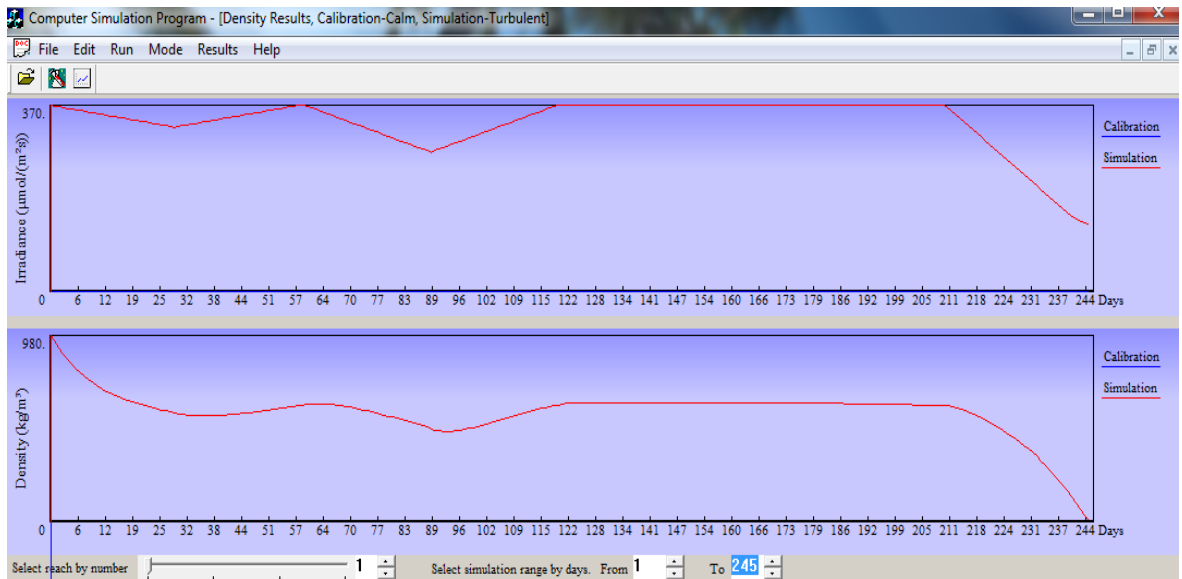


Figure 4.11. Simulation of colony density for the Riva River: Reach B and A.

Figure 4.12 is produced to observe the diurnal density changes of algal colonies. The model is simulated for a 5-day period. Results indicate the apparent effect of the response time of algae to the diurnal changes in irradiance, suggesting that colony density still continues to rise even in the dark period. The reason for this kind of behaviour can also be attributed to the importance of previous average irradiance, which is a component of equation 3.1.

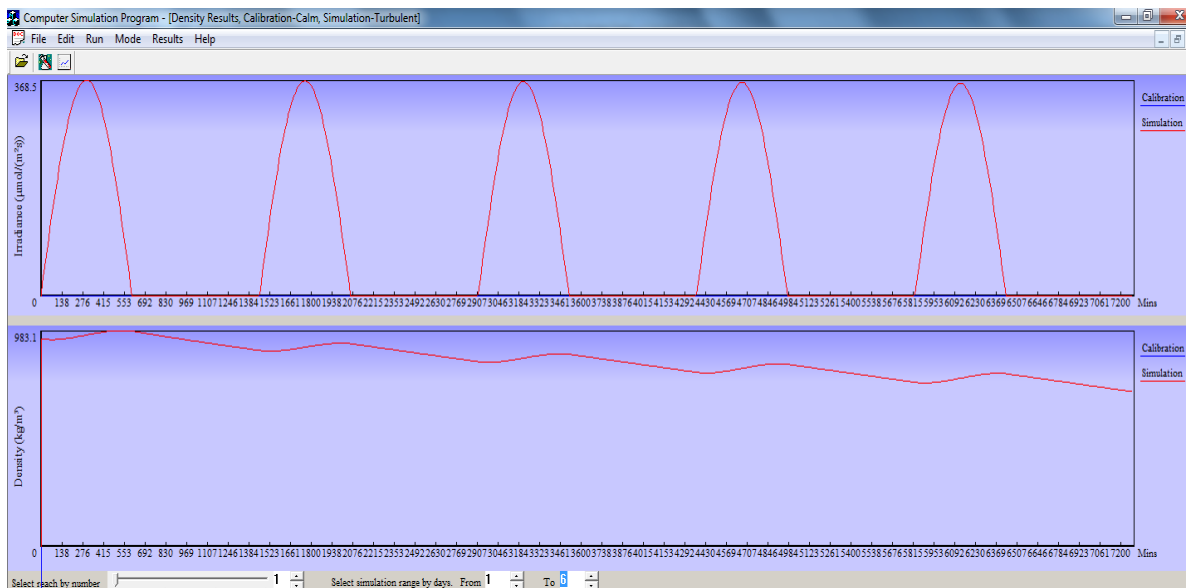


Figure 4.12. Simulation of colony density for the Riva River: Reach D and C.

### 4.2.3. Effect of Nutrient Limitation on Colony Growth

Enrichment of water bodies by nutrients is one of the key causes of algal growth, therefore it is necessary to take the effect of nutrients into account while modeling any freshwater body, which is often enriched by point or diffuse sources. Nitrogen (N) and phosphorus (P), usually in the forms of ammonia (NH<sub>4</sub>), nitrate (NO<sub>3</sub>) and phosphate (PO<sub>4</sub>), are the most dominant macro-nutrients that influence the growth of algae. Therefore, algal growth hence colony density is also a function of these nutrients up to saturation.

Phosphorus is often considered as the limiting nutrient for the growth of algae, because certain species of algae (e.g. *Anabaena* and *Aphanizomenon*) are not hindered from continued growth because of their ability of producing molecular nitrogen from the atmosphere (Kirk, 1994), a process known as nitrogen fixation. Therefore, nutrient input control usually focuses on phosphorus reduction. However, in case of river modeling, phosphorus loading from point sources may make nitrogen the limiting nutrient. The importance of nitrogen to phosphorus ratios (TN:TP) for the composition of algal blooms has been recognized for many years. For example, blue-greens are likely to dominate the growing season mean phytoplankton, when TN:TP < 29, and tend to be a minor component when TN:TP > 29 (Codd and Bell, 1985). In this study it is assumed that the algal growth is controlled by the nutrient in shortest supply, therefore ‘Liebig’s law of the minimum’ is taken into account for modeling the growth rate that depends on nutrients. This law has previously been used in algal modeling (e.g. Chapra, 1997; Klausmeier and Litchman, 2001). Liebig’s law of the minimum was applied to allow interaction between different forms of nitrogen and phosphorus, and the effect of nutrients on algal growth is represented by the following function (Equation 4.1), which is also the components of Equations 3.1 and Equation 3.7 described in the Methodology section :

$$f(N) = \min\{\alpha_N, \alpha_P\} \quad (4.1)$$

In most of the water bodies, there is a common relationship between algal blooms and total nitrogen (TN) and total phosphorus (TP). Even though, these nutrients are needed, algae requirement is not higher (NRA, 1990).

The model is run under nutrient abundant and nutrient limited conditions and Figures 4.13. and 4.14. are produced. Nutrient limited condition is given in figure 4.13, by taking into account the minimum nutrient levels observed in the Kömürlük River. For the nutrient limited simulation nitrite, nitrate and phosphate concentrations are taken as 6, 0.8 and 36 mg m<sup>-3</sup>, respectively (Tarkan, 2007). On the other hand, in Figure 4.14 it is assumed that there is no nutrient limitation. For the nutrient abundant scenario nitrite, nitrate and phosphate concentrations are taken as 22, 1 and 82 mg m<sup>-3</sup>, respectively. As can be seen from the chlorophyll-*a* levels given in Figures 4.13 and 4.14, there are no significant differences between these two nutrient conditions, as proposed with the findings of the previous literature (NRA, 1990; Howard et al., 1996).

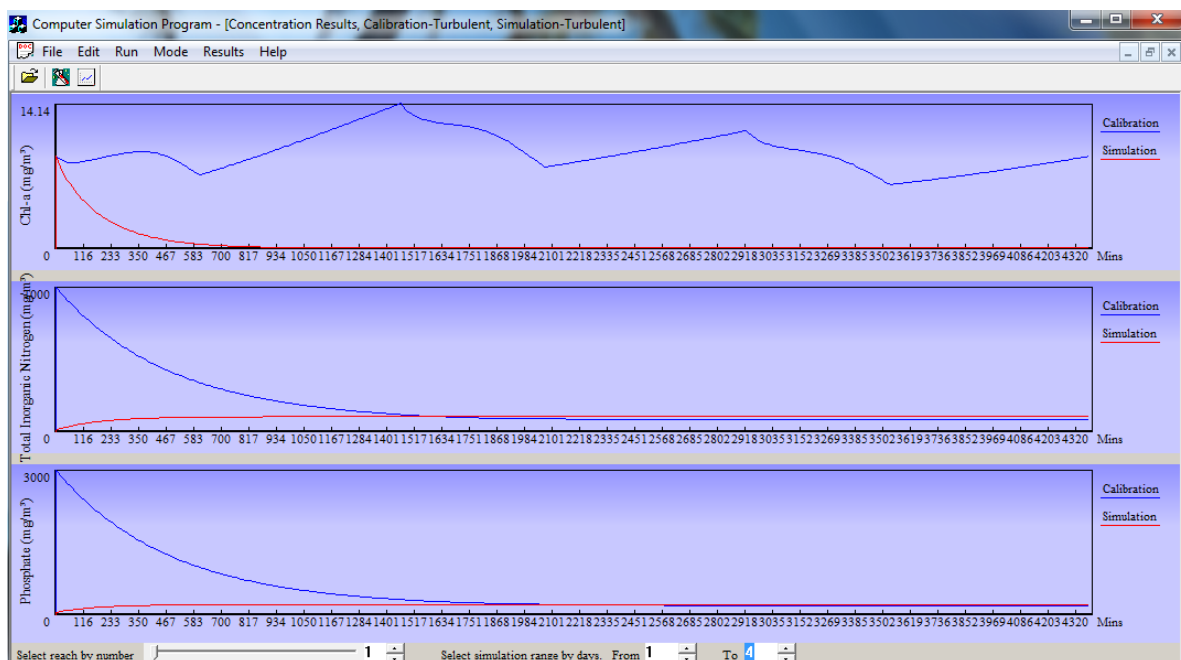


Figure 4.13. The effect of minimum nutrient conditions on colony growth in Kömürlük River Reach 1.

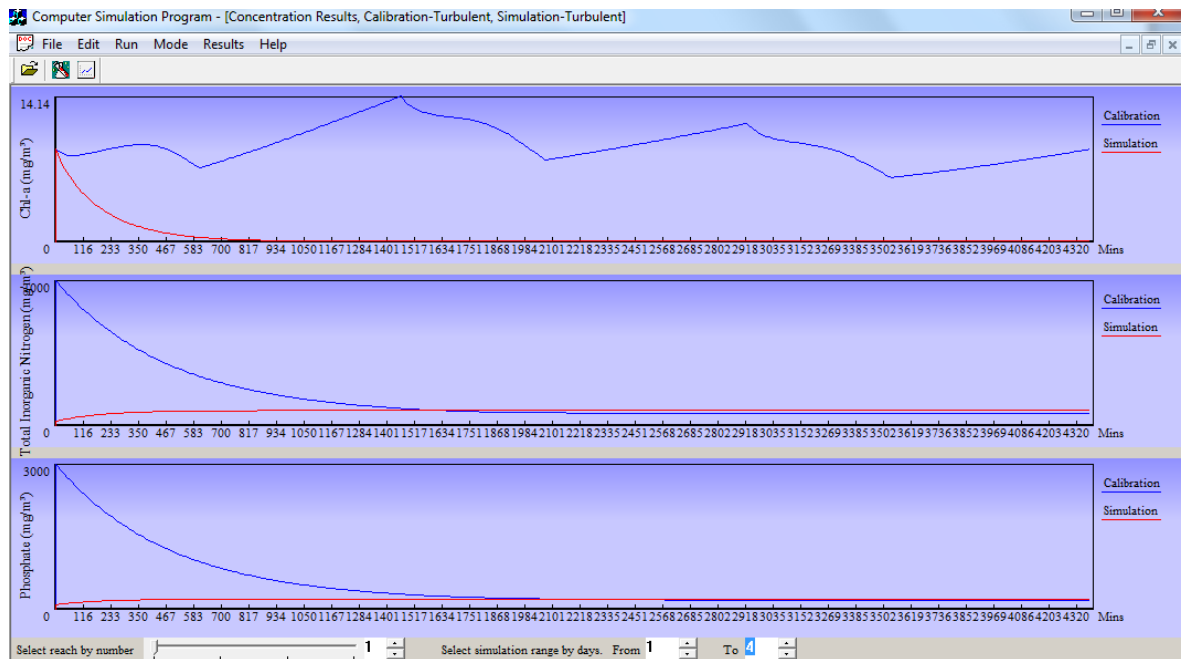


Figure 4.14. The effect of high nutrient conditions on colony growth in Kömürlük River Reach 1.

The same procedure is carried out for the Riva River and Figures 4.15 and 4.16 are produced for nutrient limited and abundant conditions, respectively. For the nutrient limited simulation nitrite, nitrate and phosphate concentrations are taken as 43, 0.9 and 719  $\text{mg m}^{-3}$ , respectively (Tarkan, 2007). Nutrient abundant scenario assumes that nitrite, nitrate and phosphate concentrations are 485, 2.87 and 2407  $\text{mg m}^{-3}$ , respectively.

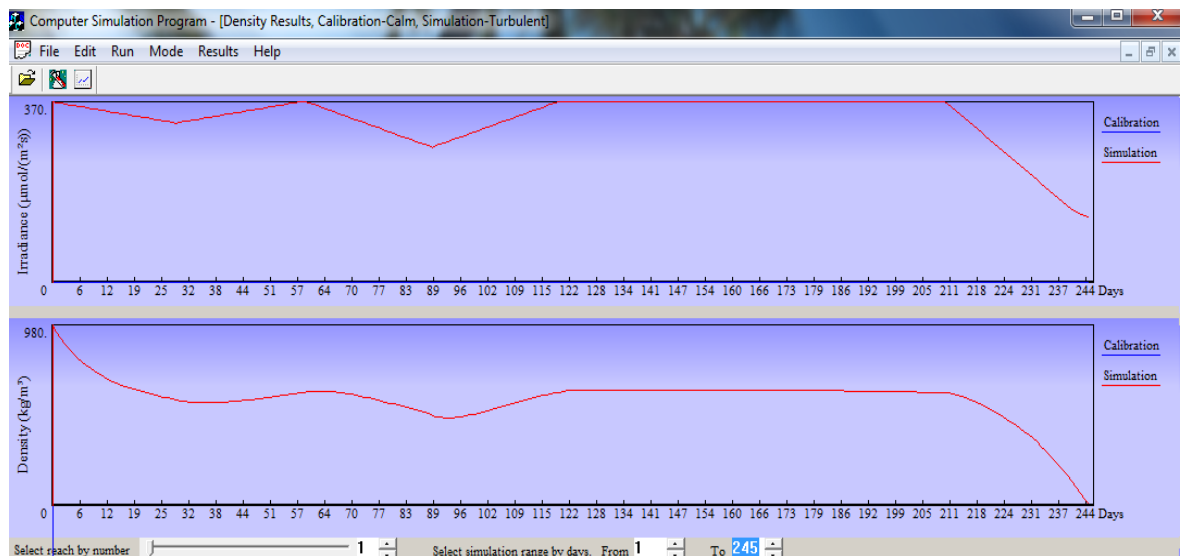


Figure 4.15. Simulation of colony density for the Riva River: Reach 2 (under low nutrient conditions).

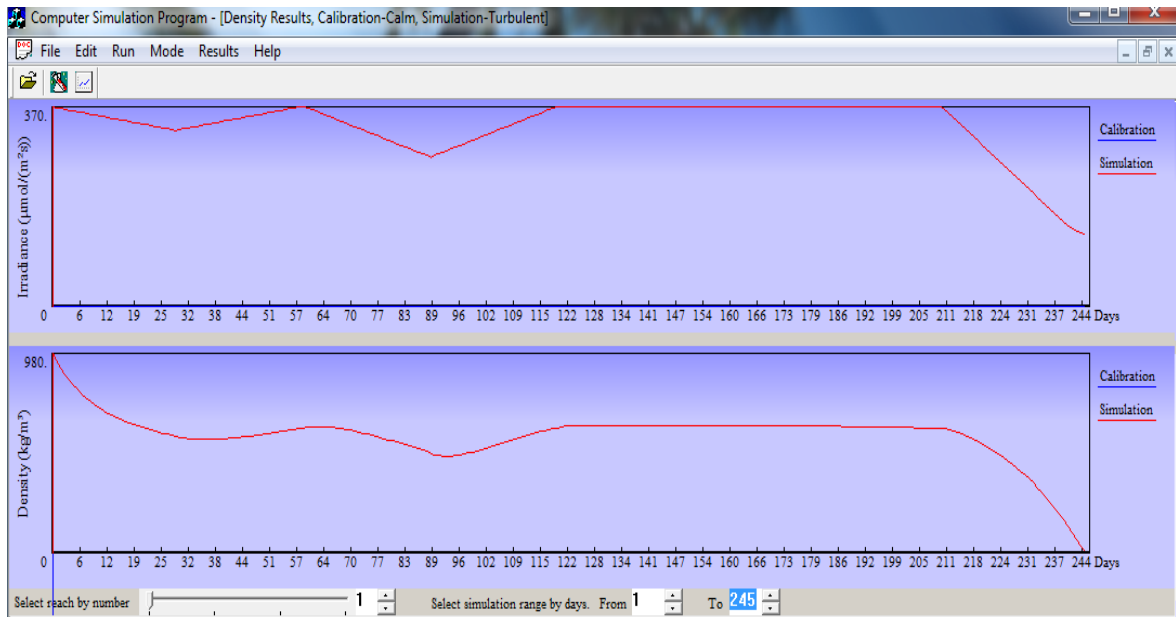


Figure 4.16. Simulation of colony density for the Riva River: Reach 2 (under high nutrient conditions).

For the Paşaköy River, colony density simulation under nutrient limited condition is provided in Figure 4.17, with the simulation values of 96, 1 and 1461  $\text{mg m}^{-3}$ , for nitrite, nitrate and phosphate concentrations, respectively (Tarkan, 2007). Because of the municipal and industrial wastewater discharges originating from the neighbouring towns of Sarıgazi, Samandıra, Alemdağ, Yenidoğan, Taşdelen and Sultanbeyli District; Paşaköy River is the most polluted and nutrient rich river amongst the 3 modeled streams (Tarkan, 2007). The rationale behind the selection of Reach 1 for model simulation for the Paşaköy River is mainly due to TP, o- $\text{PO}_4$ , and  $\text{NO}_2$  concentrations in Reach 1 being higher than Reach 2 (see Figure 3.1) (Tarkan, 2010). According to that, the high nutrient conditions for nitrite, nitrate, and phosphate are taken as 724.5, 8.5 and 4982  $\text{mg m}^{-3}$ , respectively. This extreme case can easily be observed in Figure 4.18 for nutrient abundant condition. As the figure suggests, density values predicted by the model for the Paşaköy River River are well above the values predicted for the Kömürlük and Riva Rivers. This result also explains why the algal blooms are mostly seen in the Paşaköy River due to the nutrient enrichment of the water body as a consequence wastewater discharges and being in a high urbanization zone.

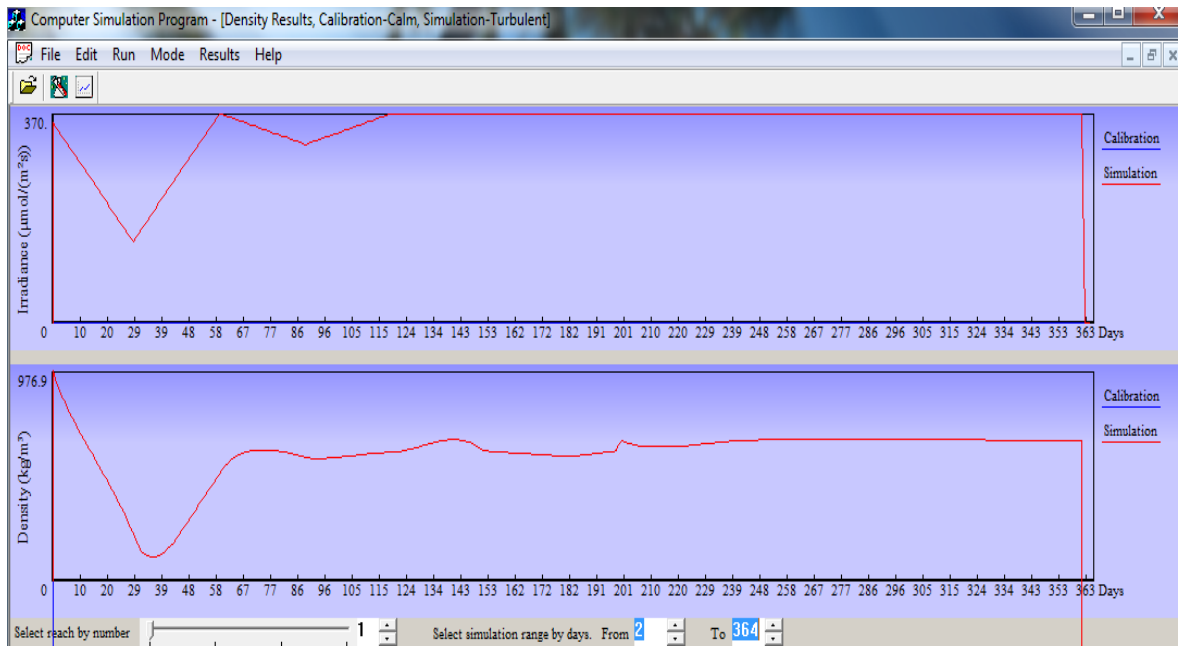


Figure 4.17. Simulation of colony density for the Paşaköy River: Reach 1 (under low nutrient conditions).

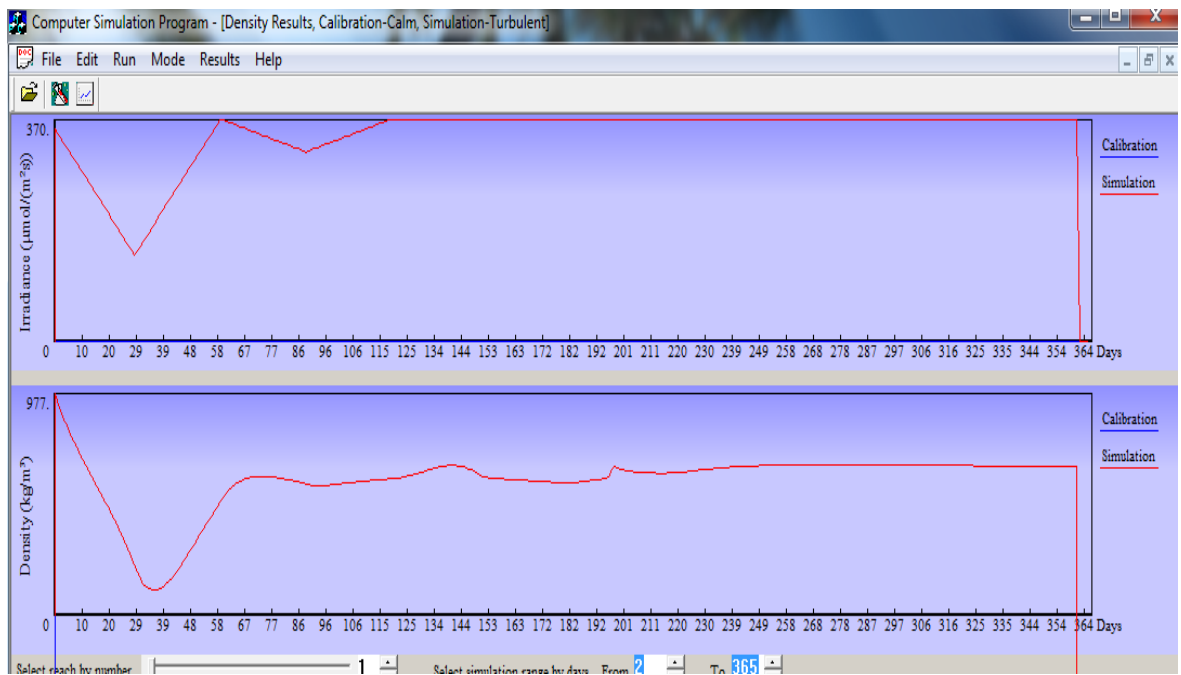


Figure 4.18. Simulation of colony density for the Paşaköy River: Reach 1 (under high nutrient conditions).

### 4.3. Results of the Movement Model

The movement of algal colonies follow an oscillatory pattern due to the diurnal changes in solar irradiance and density change. Buoyant density change in algal cells as described by Equation 1 affects the vertical migration velocity (Equation 3.2) of the colonies, which in turn determines the depth of the colony.

Figure 4.19 illustrates the oscillatory pattern of an algal colony vertical movement in a laminar flow river. The vertical migration occurs until the colony density reaches the surrounding water density. As the cells begin to receive enough irradiance at the upper layers water column, carbohydrate accumulation occurs resulting in an increase in the overall density of algae and colony sinks.

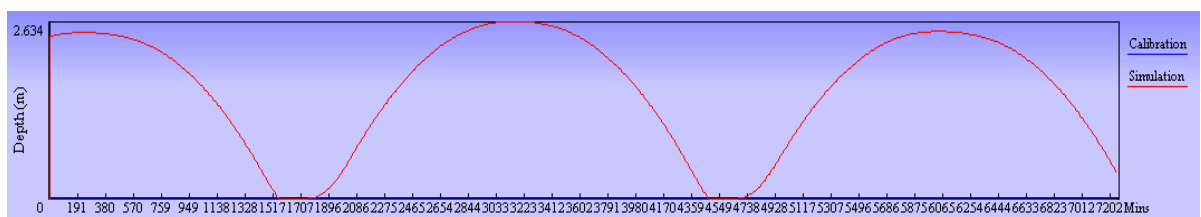


Figure 4.19. Simulation of colony depth for the Riva River: Reach 1.

In nature, algal colonies are additionally subject to the direct effects of thermal stratification in lakes and turbulence in rivers, which in turn affect the other factors, such as the availability of light (Reynolds and Walsby, 1975). Since most rivers are naturally turbulent environments, it is worthwhile to see the effect of mixing on algal behaviour. Figure 4.20 provides the vertical movement and velocity of a colony in a river for a 5-day period, where flow is dominated by the effect of turbulence. It can be seen from the graph that due to the mixing generated by the turbulence, vertical migration of algae is highly affected. According to the model (Equation 3.5), turbulence is assumed to trigger fluctuating velocities in both directions, namely in vertical and horizontal, hence retards the extreme fluctuations in the vertical oscillation of the colonies. Also, when the colony attains the water density as shown in the figure, vertical migration cannot eventuate.

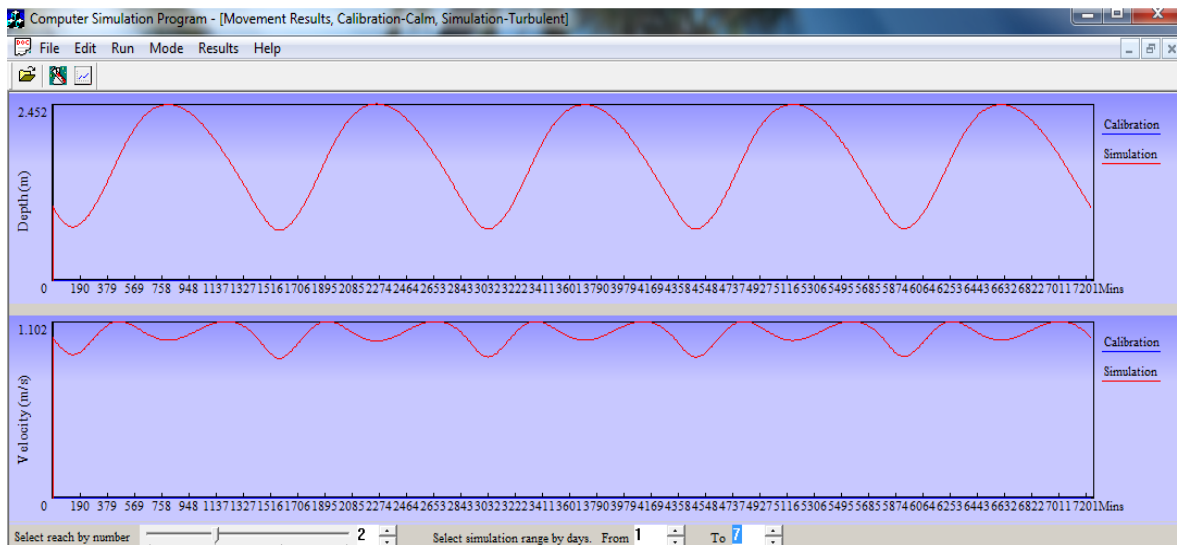


Figure 4.20. Simulation of colony depth for the Riva River Reach 1.

To demonstrate the effect of mixing further, the model is run under both calm and turbulent river conditions. In Figure 4.21, calm and turbulent flow conditions are indicated with blue and red colours, respectively. Two inferences can be drawn from the simulation. Firstly, vertical migration is hindered by turbulence, and secondly, the horizontal distances traveled by a unit colony in turbulent waters are longer than that in calm waters. In turbulent waters the horizontal fluctuating velocity adds up to the mean river velocity, causing the algaeto move faster in the lateral direction. This also explains why algal blooms tend to accumulate at downstream reaches of the rivers with relatively high flows. The vertical migration velocity in calm rivers stabilizes to some extent by the vertical fluctuating velocity component generated by turbulence, reducing the oscillation height of a unit colony. As can be seen in Figure 4.21 there is a clear separation between the depths attained by algae under calm and turbulent water conditions. Turbulent water movements tend to homogenize the population throughout the depth of mixing, so that algae may not be receiving optimal illumination at any given time (Reynolds and Walsby, 1975). When the depth of mixing exceeds the depth of the eutrophic zone, colonies spend more of their time in darkness; therefore, the average rate of photosynthetic production per unit of population is reduced (Talling, 1971).

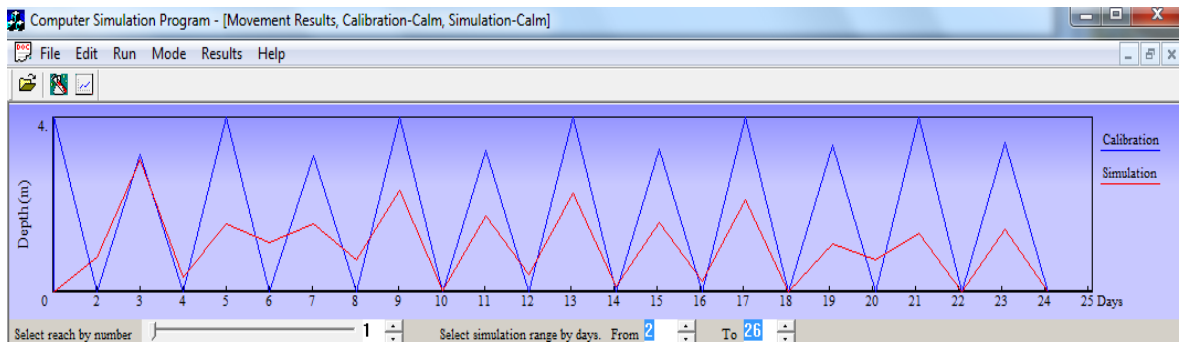


Figure 4.21. Simulation of colony depth for the K m rl k River: Reach 1.

Another prominent outcome that can be observed from the simulations is that the effect of sea tide in Reach A of the Riva River (Figure 4.22a), which is the closest station to the Black Sea, was distinctively different from simulation done for Reach G (Figure 4.22b). As figure indicates, turbulent mixing is more dominant in Reach A, because of the intrusions of the sea water to the inner part of the river mouth. As a result of velocity fluctuations generated by the turbulence, the sinking and floating extremes are hindered; thus, the depth attained by the colonies in Reach A (Figure 4.22a) becomes much lower than the depth attained by the colonies in Reach G. These results agree well with the previous findings of Temel (2006), as well.

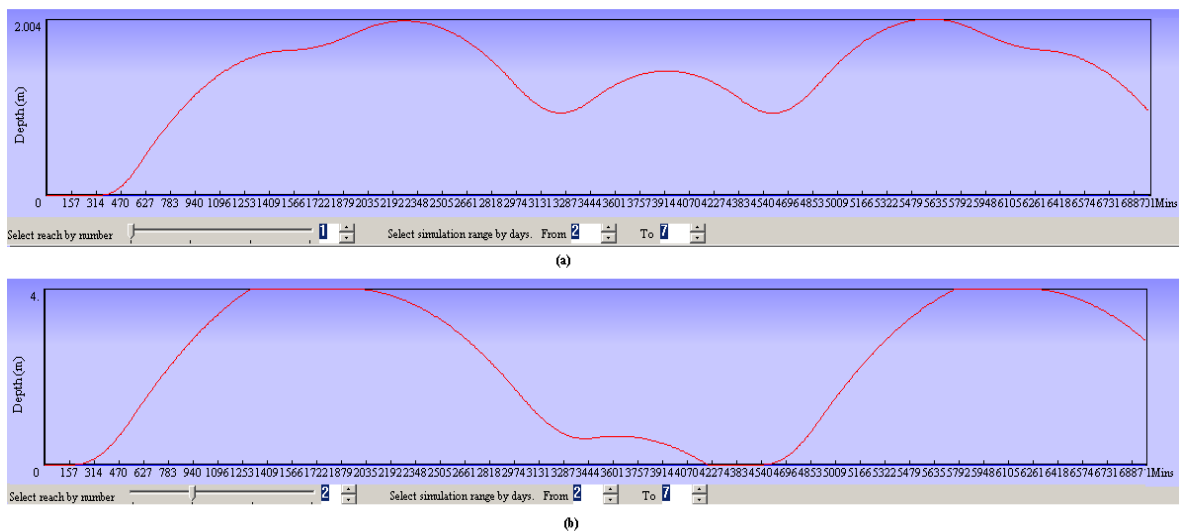


Figure 4.22. Simulation of colony depth for the Riva River: (a) Reach A, and (b) Reach G.

#### 4.4. Simulated vs. Measured Chl-*a* Results

It is important to assess the validity of the model by comparing the simulated results with the real field data. The model validation is undertaken both, based on a visual comparison by using the simulation and observed Chl-*a* graphs, and by using a statistical validation carried out with the Pearson Correlation Coefficient. Figure 4.23 and 24 shows the yearly simulations for the K m rl k and Pařak y Rivers, respectively. It is clear from the graph that Chl-*a* concentration significantly begins to increase in early spring reaching to its highest levels around summer season. This seasonal pattern is of course a consequence of the increase in photosynthetic activity as a result of solar irradiance.

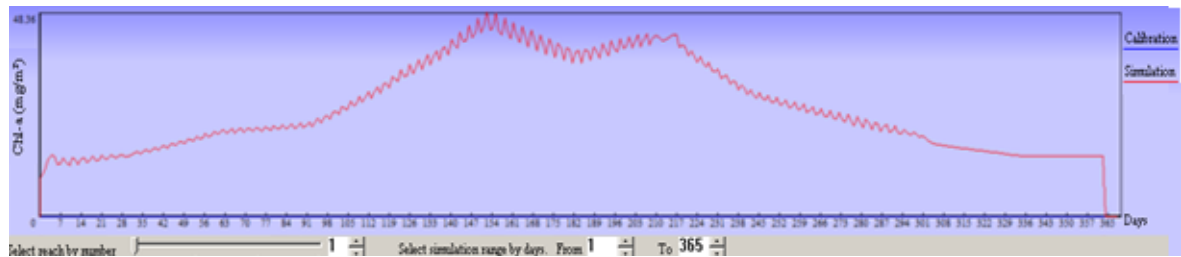


Figure 4.23. Simulation of Chl-*a* for the K m rl k River: Reach 1.

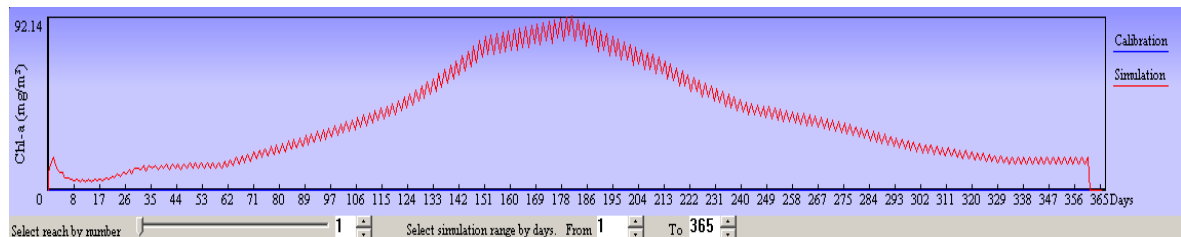


Figure 4.24. Simulation of Chl-*a* for the Pařak y River: Reach 1.

Moreover, it is clear from the above simulations that (Figure 4.23 and 4.24), there is a significant difference between the Chl-*a* concentrations belonging to the K m rl k and Pařak y Rivers. This is also a consequence and an indicator of the lower TN:TP ratio calculated from data provided by Tarkan (2006), for the Pařak y River. TN:TP ratio calculated for the K m rl k River was approximately three times higher than the ratio for the Pařak y River. A TN:TP decrease is usually observed during lake eutrophication process, and a low TN:TP is also associated with human induced nutrient loads to freshwaters. One of the main reasons behind this condition is that, as also briefly discussed previously in Section 4.2.3, N originates from atmosphere as an inert gas. This also

explains why, both  $N_2$  –fixing cyanophytes and bloom-forming algae usually dominates freshwaters with relatively low TN:TP ratios. From these aspects, increased urbanization and domestic wastewater discharge to the stream makes Paşaköy River more vulnerable to eutrophication and algal blooming.

In order to be able to observe the monthly change in Chl-*a*, the model is run for a year from June to the July of the following year. The rationale behind this was to observe whether the similar pattern was occurring in two subsequent years, 2005 and 2006, around summer months, and also to observe the harmony between predicted and measured Chl-*a* concentrations. Figures 4.25 and 4.26, illustrates the modeled and measured Chl-*a* concentrations for the Paşaköy River, Reach 1, respectively. Although there is not a perfect quantitative match between the simulated and measured concentration values, from the figures below, it is possible to conclude that the model is capable in predicting the seasonal trend and extremes, indicating that the model would be successful in predicting the timing of possible algal blooming event occurrence in the river.

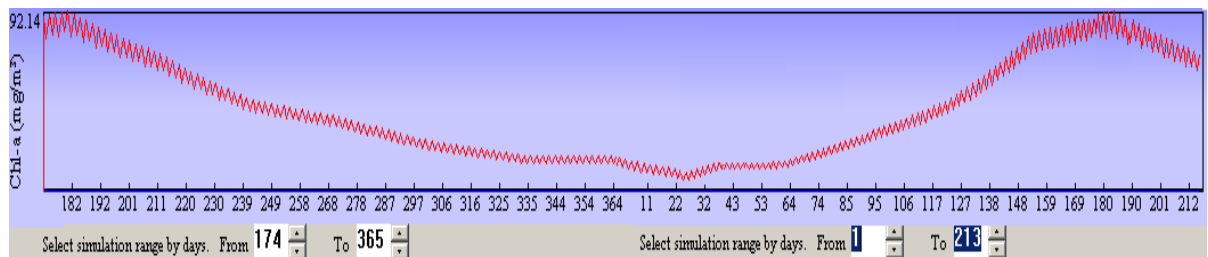


Figure 4.25. Simulation of Chl-*a* for the Paşaköy River: Reach 1.

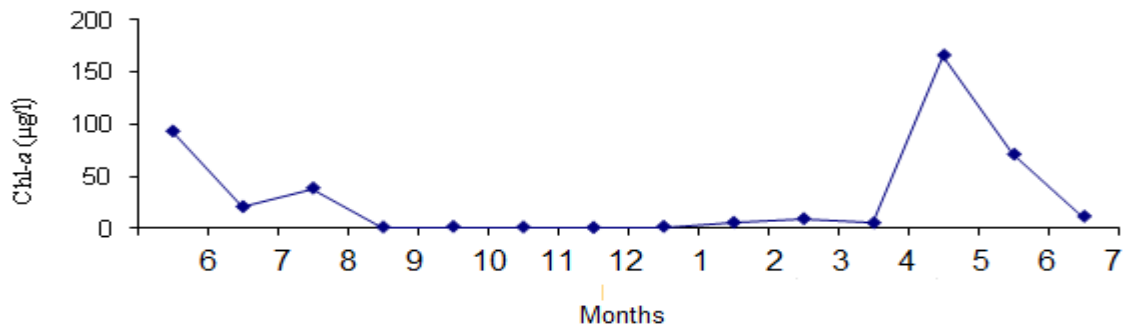


Figure 4.26 Measured Chl-*a* for the Paşaköy River: Reach 1.

For the statistical validation, Pearson correlation is used, which is a measure of the linear dependence between two variables. The analysis is done for the K m rl k River, Reach 1, between modeled and real data as provided in Figure 4.27. Results indicates a reasonable model validation, that the simulated chl-a values are positively correlated to the measured chl-a values, with a Pearson correlation coefficient of 0.77 ( $r = 0.77$ ).

Figure 4.27 illustrates a qualitative comparison of the simulated and measured monthly Chl-*a* concentrations for the K m rl k River. According to the figure the model has a fairly good seasonal prediction trend of Chl-*a* for the K m rl k River, having the highest trends between spring and autumn, which can be attributed to the effect of increasing irradiance and temperature values that enhance the photosynthetic activity of the algae. It should be noted that the model is more capable in providing seasonal prediction of blooming events, rather than predicting the intensity of algal blooms. This consequence can be attributed to several facts: Firstly, in the model, growth kinetics parameters, such as the maximum growth rate or death constants were taken for the *Microcystis* sp., whereas analyzed water quality samples included mixed species (Temel, 2006). Secondly, although being an important component of algal growth, there were no ammonium concentration data available for the simulations. Moreover, as with any model application, there were some assumptions made for missing data, such as initial algal biomass, which may hinder a better quantitative match. Despite these limitations regarding data, Figure 4.27 suggests that the mechanistic structure of the model makes it adequate for simulations of seasonal bloom prediction.

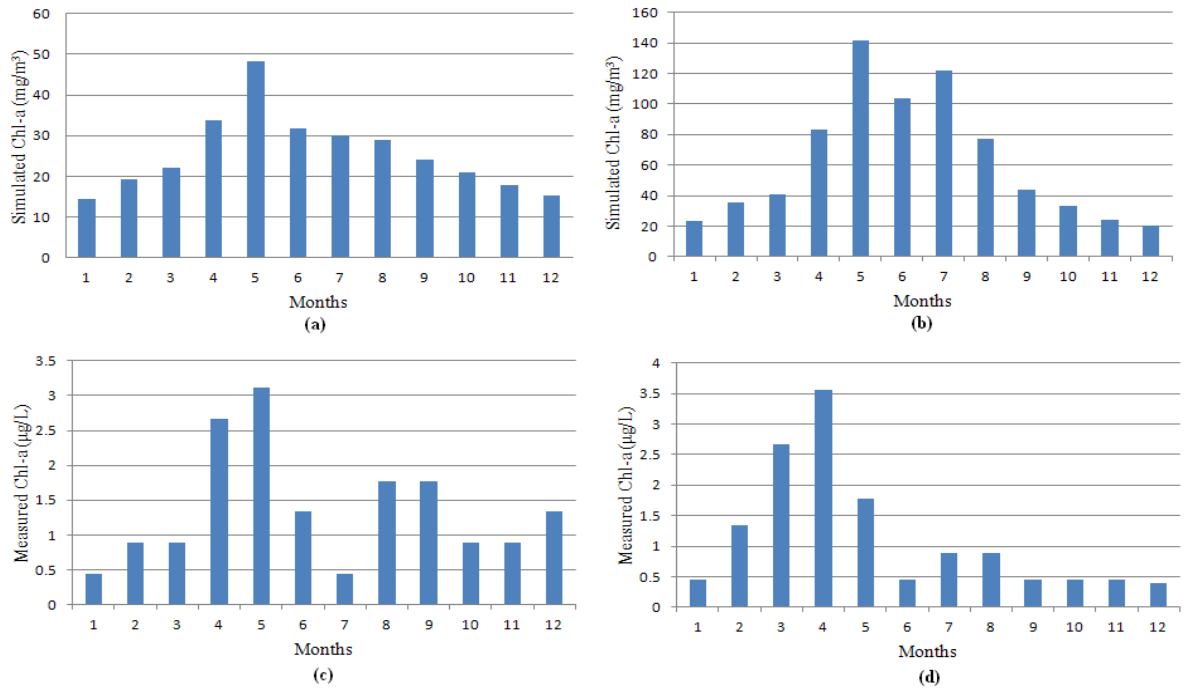


Figure 4.27. Simulated vs. Measured Chl-*a* concentrations for the Kömürlük River (a) simulated Chl-*a* concentrations in Kömürlük River, Reach 1 (b) simulated Chl-*a* concentrations in Kömürlük River, Reach 2 (c) measured Chl-*a* concentrations in Kömürlük River, Reach 1 (d) measured Chl-*a* concentrations in Kömürlük River, Reach 2.

## 4. CONCLUSIONS AND RECOMMENDATIONS

Understanding algal behaviour, especially in terms of growth and transport, is a need for predicting the intensity, timing and location of future bloom events. Computer simulation models can be useful tools in managing the eutrophication problem associated with excess growth of algae. In an attempt to provide an example to such an application, a formerly developed theoretical model (Güven and Howard, 2006b) is applied to three streams of the Ömerli Reservoir.

When developing deterministic-mathematical models, usually the emphasis is given to the correct formulation of the theoretical model algorithms. This approach sometimes may lead to the underestimation of the requirement for data gathering, as it is not always possible to obtain real, sufficient and reliable field data. The strength of this study is that, the dataset used for model application included comprehensive physical, chemical and biological monthly water quality data for one year for the Riva, Paşaköy and Kömürlük Streams. Other topographical data used in the model, such as elevation, slope and reach length are obtained through the GIS.

It is possible to draw several conclusions from the study presented in this thesis:

- Solar irradiance limitation has a more pronounced affect than nutrient limitation, assuming that there is no external discharge being made to the river.
- There is an annual cycle of growth for algae, usually having one or two periods in one year.
- Increased turbulence in the river hinders the accumulation of algal blooms on water surface. Light is a major source of energy for photosynthetic activity and elimination of light can be achieved by manipulating the light conditions, for example by artificial mixing of the water column. Vertical migration of algal colonies due to the changes in their buoyant state as a result of photosynthetic activity, usually occurs under calm conditions.

- The simulated Chl-*a* values are positively correlated to the measured values with a Pearson correlation coefficient of 0.77.

Under favorable environmental conditions such as the availability of adequate light, nutrients, and temperature, water bodies may suffer from toxic algal blooms, especially in spring and mid-summer. This situation may even get worse as a result of increased pollution or climate change. In this study, this effect was the most distinguished in the Paşaköy Stream, probably as a consequence of municipal and industrial wastewater discharges originating from the neighbouring towns, as well as increased urbanization around the river.

Process-based mathematical modeling is a helpful tool for managing aquatic environments for sustaining better status. According to MacKay et al. (1995), mathematical models are best used to describe physical systems that tend to behave in a highly repeatable manner, such as the growth and movement of patterns of algal colonies, which follow an oscillatory, sinusoidal pattern as a result of the diurnal changes in solar irradiance and density change. Results indicated that the model predictions are quite reasonable in terms of expressing the relationships between environmental variables such as, irradiance, nutrient, temperature, turbulence, and algal density change. Furthermore, the simulations also indicate an acceptable prediction of seasonal Chl-*a* concentrations. Therefore, process-based mathematical models can be used to predict the likely future behaviour of algae, and would be useful tools in eutrophication control and management, and associated bloom prediction in river-style reservoirs, such as the Ömerli Reservoir.

Future blooming events are likely to be affected by changing precipitation patterns and increasing temperature, which act as governing forcing functions for algae growth. When supported by reliable data, the outcomes of such modeling studies can be used by water quality managers for the early warning of problems associated with eutrophication.

## REFERENCES

- Albay, M., Akçaalan, R., 2003. Factors influencing the phytoplankton steady state assemblages in a drinking water reservoir, Ömerli reservoir, Istanbul. *Hydrobiologia*, 502, 85-95.
- Allison, E.M., Walsby, A.E., 1981. The role of potassium in the control of turgor pressure in a gas-vacuolate blue-green alga. *Journal of Experimental Botany*, 32, 241-249.
- Bannister, T.T., 1979. Quantitative description of steady state, nutrient-saturated algal growth, including adaptation. *Limnology Oceanography*, 24, 76-96.
- Belov, A.P., Giles, J.D., Wiltshire, R.J., 1999. Toxicity in a water column following the stratification of a cyanobacterial population development in a calm lake. *IMA Journal of Mathematics Applied in Medicine and Biology*, 16, 93-110.
- Bingham, D.R., Lin, C., Hoag, R.S., 1984. Nitrogen cycle and algal growth modelling. *Journal the Water Pollution Control Federation*, 56, 1118-22.
- California Regional Water Quality Control Board North Coast Region, 2009. <http://www.cdph.ca.gov/HealthInfo/environhealth/water/Documents/BGA/RegionalBoardBGAPressRelease-08-2009.pdf> (accessed May 2012).
- Carmichael, W.W., Callow, J.A. (Eds), 1986. Algal toxins, in *Advances in Botanical Research*. Academic Press, London, 47-101.
- Chapra, S.C., 1997. *Surface water-quality modeling*. McGraw-Hill International editions, 603, 21.
- Chorus, I., Bartram, J., 1999. *Toxic Cyanobacteria in water: A Guide to Their Public Health Consequences Monitoring and Management*, London.
- Cloot, A., Roux, G.L., 1997. Modelling algal blooms in the middle Vaal River, a site specific approach. *Water Research*, 31, 2, 271-279.

Codd, G.A., Bell, S.G., 1985. Eutrophication and Toxic Cyanobacteria in Freshwaters. *Water Pollution Control*, 84, 225-232.

Codd, G.A., Poon, G.K., Rogers, L.J., Gallon, J.R. (Eds), 1988. Cyanobacterial toxins In *Biochemistry of the algae and cyanobacteria*. Europe, Oxford University Press, Oxford, 28, 283-296.

De Boer, B., 1979. A moving cell model of the dissolved oxygen and phytoplankton Dynamics in rivers. *Hydrological Sciences*, 24, 199-211.

Dinseven, E., Çurgunlu, E., 1988. Determination of the throphic status of the Riva Stream for monitoring eutrophication. *Su Ürünleri dergisi*, 2, 2, 35-52.

Fadel,A., Bruno, L.,Brigitte, V.L., 2011. A coupled hydrodynamic biological model for cyanobacteria dynamics in reservoirs, 11th edition of the World Wide Workshop for Young Environmental Scientists, France.

Falconer, I.R., 1989. Effects on human health of some toxic cyanobacteria, blue-green algae, in reservoirs, lakes, and rivers. *Toxicity Assessment*, 4, 1175-84.

Ferguson, A.J.D., 1997. The role of modelling in the control of toxic blue green algae. *Hydrobiologia*, 349, 1-4.

Fogg, G.E., 1969. The physiology of an algal nuisance. *Proceedings of the Royal Society of London*. 173, 175-189.

Fogg, G.E., Stewart, W.D.P., Fay, P., Walsby, A.E., 1973. *The Blue-green Algae*. London and New York Academic Press.

Frisk, T., Bilaletdin, Ä., Kaipainen, H., Malve, O., Möls, M., 1999. Modelling phytoplankton dynamics of the eutrophic Lake Võrtsjärv, EstoniA. *Hydrobiologia*,414, 59-69.

Grant, N.G., Walsby, A.E., 1977. The contribution of photosynthate to turgor pressure rise in the planktonic blue-green alga *Anabaena flos-aquae*. *Journal of Experimental Botany*, 28, 409-415.

Güven, B., Howard, A., 2006a. A review and classification of the existing models of cyanobacteria *Progress in Physical Geography*, 30-1.

Güven, B., Howard, A., 2006b. Modelling the growth and movement of cyanobacteria in river systems. *Science of the Total Environment*, 368, 898–908.

Güven B., Howard A. 2007. Identifying the critical parameters of a cyanobacterial growth and movement model by using generalised sensitivity analysis, *Ecological Modelling*, 207, 11-21.

Hiroshi, S., Takashi, A., Axel, G., Kiminori, I., 2008. Computer simulations of seasonal outbreak and diurnal vertical migration of cyanobacteria. *Limnology*, 9, 185–194.

Howard, A., 1993. SCUM simulation of cyanobacterial underwater movement. *Computer Application in the Bioscience*, 9, 413–9.

Howard, A., 1993. Modelling the movement and growth of freshwater cyanobacterial blooms. PhD thesis, The University of Leeds.

Howard, A., Irish, A.E, Reynolds, C.S., 1996. A new simulation of cyanobacterial underwater movement (SCUM'96). *Journal of Plankton Research*, 18, 1375–85.

Ibelings, B.W., Mur, L.R., Walsby, A.E., 1991. Diurnal changes in buoyancy and vertical distribution in populations of *Microcystis* in two shallow lakes. *Journal of Plankton Research*, 13, 419–436.

Jeong, K.S., Kim, D.K., Whigham, P., Joo, G.J., 2003. Modelling *Microcystis aeruginosa* bloom Dynamics in the Nakdong River by means of evolutionary computation and statistical approach. *Ecological Modelling*, 161, 67-78.

Jöhnk, K.D., Brüggemann, R., Rucker, J., Luther, B., Simon, U., Nixdorf, B., Wiedner, C., 2011. Modelling life cycle and population dynamics of Nostocales, cyanobacteria. *Environmental Modelling and Software*, 26, 669-677.

Kinniburgh, J.H., Barnett, M., 2010. Orthophosphate concentrations in the River Thames, reductions in the past decade. *Journal of Water Environment*, 24, 107–115.

Kirk, J.T.O., 1994. Light and photosynthesis in aquatic ecosystems. Cambridge University Press, 339.

Klausmeier, C.A., Litchman, E., 2001. Algal games: The vertical distribution of phytoplankton in poorly mixed water columns. *Limnology Oceanography*. 46, 8, 1998-2007.

Kristov, J., Sigeo, D., Corliss, J., and Bellinger, E., 1999. Examination of the phytoplankton of Rostheme Mere using a simulation mathematical model. *Hydrobiologia*, 414, 71-76.

Kromkamp, J., Mur, L.R., 1984. Buoyant density changes in the cyanobacterium *Microcystis aeruginosa* due to changes in the cellular carbohydrate content. *FEMS Microbiology Letters*, 25, 105-109.

Kromkamp, J., Walsby, A.E., 1990. A computer model of buoyancy and vertical migration in cyanobacteria. *Journal of Plankton Research*, 12, 161–83.

Laws, E.A., Challup, M.S., 1990. A microalgal growth model. *Limnology Oceanography*, 35, 3, 597-608.

- Lung, W.S., Paerl, H.W., 1988. Modelling blue-green algal blooms in the lower Neuse River. *Water Research*, 22, 7, 895-905.
- MacKay, D., Burns, L.A., Rand, G.M., 1995. *Fate Modeling*. Taylor & Francis, Bristol, Pennsylvania, 563-586.
- Maier, H.R., Dandy, G.C., 1997. Modelling cyanobacteria, blue-green algae, in the River Murray using artificial neural networks. *Mathematics and Computers in Simulation*, 43, 377-386.
- National Rivers Authority, 1990. *Toxic Blue-Green Algae*. Water Quality Series, London, 2.
- Negri, A.P., Jones, G.J., Hindmarsh, M., 1995. Sheep mortality associated with Paralytic Shellfish poisoning toxins from the cyanobacterium *Anabaena circinalis*. *Toxicon*, 33, 1321-1329.
- O'Brien, W.J., 1974. The dynamics of nutrient limitation of phytoplankton algae, A model reconsidered. *Ecology*, 55, 1, 135-141.
- Okada, M., Aiba, S., 1983a. Simulation of water-bloom in a eutrophic lake-II. *Water Research*, 17, 8, 877-882.
- Okada, M., Aiba, S., 1983b. Simulation of water-bloom in a eutrophic lake-III. *Water Research*, 17, 8, 883-893.
- Oslon, J.M., 2006. Photosynthesis in the Archean era. *Photosynthesis Research*, 88, 2, 109-17.
- Pouria, S., Andrade, A., Barbosa, J., Cavalcanti, R.L., Barreto, V.T., Ward, C.J., 1998. Fatal microcystin intoxication in haemodialysis unit in Caruaru, Brazil. *Lancet*, 352, 21-6.

Pretty, J.N., Mason, C.F., Nedwell, D.B., Hine, R.E., 2002. A Preliminary Assessment of the Environmental Costs of the Eutrophication of Fresh Waters in England and Wales. University of Essex, 56.

Recknagel, F., 1997. ANNA, Artificial Neural Network model for predicting species abundance and succession of blue green algae. *Hydrobiologia*, 349, 47-57.

Reynolds, C.S., Walsby, A.E., 1975. Water blooms. *Biological Reviews*, 50, 437-481.

Reynolds, C.S., 1987. Cyanobacterial water blooms. In: J.A. Callow Ed. *Advances in Botanical Research*. Academic Press, London, 68-143.

Reynolds, C.S., Oliver, R.L., Walsby, A.E., 1987. Cyanobacterial dominance the role of buoyancy regulation in dynamic lake environments. *New Zealand Journal of Marine and Freshwater Research*, 21, 379-390.

Reynolds, C.S., Irish, A.E., 1997. Modelling phytoplankton dynamics in lakes and reservoirs, the problem of in-situ growth rates. *Hydrobiologia*, 349, 5-17.

Sigeo, D.C., 2005. *Freshwater microbiology*. John Wiley and Sons Ltd, West Sussex.

Talling, J.F., 1971. The underwater light climate as a controlling factor in the production ecology of freshwater phytoplankton. *Mitteilungen der internationale Vereinigung für theoretische und angewandte, Limnologie*. 19, 214-43.

Tarkan, S.A., 2007. Investigations of some physical, chemical and biological features of Streams which flow into Ömerli Reservoir, Ph.D. Thesis, İstanbul University, Fisheries Faculty.

Tarkan, S.A., 2010. Effect on streams on drinkable water reservoir: an assessment of water quality, physical habitat and some biological features of the streams. *Journal of Fisheries Science*, 4, 1, 8-19.

- Temel, M., 1994. Riva deresi fitoplanktonu üzerinde bir ön araştırma (A preliminary study on phytoplankton of Riva Stream). I.Ü. Su Ürünleri Dergisi, 8,1-2, 1-15.
- Temel, M., 2006. A study on Prokaryota Cyanobacteria, Cyanoprokaryota, and Eukaryota algae in the Riva Stream, Istanbul, Turkey. Hydrobiologia, 8, 79-90.
- Thebault, J.M., Qotbi, A., 1999. A model of phytoplankton development in the Lot River, France. Simulations of scenarios. Water Research, 33, 4, 1065-1079.
- Visser, P.M., Passarge, J., Mur, L.R., 1997. Modelling vertical migration of the cyanobacterium *Microcystis*. Hydrobiologia, 349, 99-109.
- Wallace, B.B., Hamilton, D.P., 1999. The effect of variations in irradiance on buoyancy regulation in *Microcystis aeruginosa*. Limnology Oceanography, 42, 2, 273-281.
- Wallace, B.B., Hamilton, D.P., 2000. Simulation of water-bloom formation in the cyanobacterium *Microcystis aeruginosa*. Journal of Plankton Research, 22, 6, 1127-1138.
- Walsby, A.E., 1970. The nuisance algae: curiosities in the biology of planktonic blue-green algae. Water Treatment and Examination, 19, 359-373.
- Walsby, A.E., 1971. The pressure relationships of gas vacuoles. Proceedings of the Royal Society of London B. 178, 301-326.
- Walsby, A.E., 1994. Gas vesicles. Microbiological Reviews, 58, 94-144.
- Whitehead, P.G., Hornberger, G.M., 1984. Modelling algal behaviour in the River Thames. Water Research, 18, 8, 945-953.
- Whitehead, P.G., Williams, R.J., Lewis, D.R., 1997. Quality simulation along river systems, QUASAR, model theory and development. The Science of the Total Environment, 194,195, 447-456.

Young, G.K., Asce, M., Saunders, K.G., 1985. Phosphorus reduction for control algae. *Journal of Environmental Engineering*, 111, 574-88.

Zevenboom, W., Mur, L.R., 1984. Growth and photosynthetic response of the cyanobacterium *Microcystis aeruginosa* in relation to photoperiodicity and irradiance. *Archives of Microbiology*, 139, 232-239.

**APPENDIX A: SCREENSHOTS OF THE ‘EDIT PARAMETERS’ MENU OF THE MODEL SHOWING THE DATA FOR THE FIRST REACHES OF THE RİVA, PAŞAKÖY AND KÖMÜRLÜK RIVERS**

The screenshot shows a software window titled 'Edit Parameters' with a tabbed interface. The 'Reach1' tab is selected, and within it, the 'Variables' sub-tab is active. The window contains a grid of parameter labels and input fields with numerical values. At the bottom, there are three buttons: 'Tamam', 'İptal', and 'Uygula'.

Parameter	Value	Parameter	Value
Initial colony depth (m)	1.	Water density (kg/m <sup>3</sup> )	1000.
Initial colony density (kg/m <sup>3</sup> )	980.	Hydraulic radius (m)	1.
Day length (min)	600.	Slope of energy gradeline	5.e-004
Ammonium concentration (mg/m <sup>3</sup> )	0.	River depth (m)	4.
Nitrite concentration (mg/m <sup>3</sup> )	125	Surface slope	1,26
Nitrate concentration (mg/m <sup>3</sup> )	1,93	Flow (m <sup>3</sup> /s)	2
Phosphate concentration (mg/m <sup>3</sup> )	1666	Pre. ave. irradiance (μmol/(m <sup>2</sup> s))	38.
Initial biomass (mg/m <sup>3</sup> )	9.	External Nitrogen load (mg/m <sup>3</sup> )	100.
Cell volume / Colony volume	1.	External Phosphorus load (mg/m <sup>3</sup> )	200.
Fom resistance	1.		
Colony radius (μm)	200.		

Figure A1. A screenshot of the computer simulation program showing the ‘Variables’ menu for Riva River Reach 1.

Edit Parameters

Reach1 | Reach2 | Reach3 | Reach4

Variables | Parameters | Monthly Data

Extinction coefficient (1/m)	2.	Manning's constant	1.
Density gain coef. (kg/(m <sup>3</sup> min))	0.132	Manning's roughness coefficient	3.e-002
Density loss coef. (kg/m <sup>3</sup> minμmolm <sup>3</sup> s)	1.67e-005	Von Karman constant	0.4
Min. rate of density dec. (kg/m <sup>3</sup> min)	2.3e-002	Zero velocity height (m)	3.5
Half-sat. constant for I (μmol/m <sup>3</sup> s)	25.	D65 (m)	0.
Half-sat. constant for N (mg/m <sup>3</sup> )	25.	Boundary rough. projection height(m)	3.e-002
Half-sat. constant for P (mg/m <sup>3</sup> )	3.	Death rate (1/d)	0.1
Reach length (m)	3785	Cross sectional area (m <sup>2</sup> )	6
Temperature activity coefficient	1.066		
Maximum growth rate (1/s)	5.5e-005		
Gravitational acceleration (m/s <sup>2</sup> )	9.81		

Tamam iptal Uygula

Figure A2. A screenshot of the computer simulation program showing the 'Parameters' menu for the Riva River, Reach 1.

Edit Parameters

Reach1 | Reach2 | Reach3 | Reach4

Variables | Parameters | Monthly Data

Temperature °C (Jan)	6.7	Irradiance $\mu\text{mol}/(\text{m}^2\text{s})$ (Jan)	370
Temperature °C (Feb)	7.4	Irradiance $\mu\text{mol}/(\text{m}^2\text{s})$ (Feb)	325
Temperature °C (Mar)	12	Irradiance $\mu\text{mol}/(\text{m}^2\text{s})$ (Mar)	370
Temperature °C (Apr)	15.2	Irradiance $\mu\text{mol}/(\text{m}^2\text{s})$ (Apr)	275
Temperature °C (May)	24.2	Irradiance $\mu\text{mol}/(\text{m}^2\text{s})$ (May)	370
Temperature °C (Jun)	24	Irradiance $\mu\text{mol}/(\text{m}^2\text{s})$ (Jun)	370
Temperature °C (Jul)	25.5	Irradiance $\mu\text{mol}/(\text{m}^2\text{s})$ (Jul)	370
Temperature °C (Aug)	27.2	Irradiance $\mu\text{mol}/(\text{m}^2\text{s})$ (Aug)	370
Temperature °C (Sep)	21.7	Irradiance $\mu\text{mol}/(\text{m}^2\text{s})$ (Sep)	147
Temperature °C (Oct)	19.1	Irradiance $\mu\text{mol}/(\text{m}^2\text{s})$ (Oct)	25
Temperature °C (Nov)	13.8	Irradiance $\mu\text{mol}/(\text{m}^2\text{s})$ (Nov)	370
Temperature °C (Dec)	10.2	Irradiance $\mu\text{mol}/(\text{m}^2\text{s})$ (Dec)	370

Tamam İptal Uygula

Figure A3. A screenshot of the computer simulation program showing the ‘Monthly Data’ menu for the Riva River, Reach 1.

Edit Parameters

Reach1 | Reach2 | Reach3 | Reach4

Variables | Parameters | Monthly Data

Initial colony depth (m)	1	Water density (kg/m <sup>3</sup> )	1000.
Initial colony density (kg/m <sup>3</sup> )	980.	Hydraulic radius (m)	1.
Day length (min)	600.	Slope of energy gradeline	1,97
Ammonium concentration (mg/m <sup>3</sup> )	0.	River depth (m)	4
Nitrite concentration (mg/m <sup>3</sup> )	96	Surface slope	1,86
Nitrate concentration (mg/m <sup>3</sup> )	1	Flow (m <sup>3</sup> /s)	2
Phosphate concentration (mg/m <sup>3</sup> )	1461	Pre. ave. irradiance (μmol/(m <sup>2</sup> s))	38.
Initial biomass (mg/m <sup>3</sup> )	9.	External Nitrogen load (mg/m <sup>3</sup> )	100.
Cell volume / Colony volume	1.	External Phosphorus load (mg/m <sup>3</sup> )	200.
Fom resistance	1.		
Colony radius (μm)	200.		

Tamam iptal Uygula

Figure A4. A screenshot of the computer simulation program showing the ‘Variables’ menu for the Paşaköy River, Reach 1.

Edit Parameters

Reach1 | Reach2 | Reach3 | Reach4

Variables | Parameters | Monthly Data

Extinction coefficient (1/m)	2.	Manning's constant	1.
Density gain coef. (kg/(m <sup>3</sup> min))	0.132	Manning's roughness coefficient	3.e-002
Density loss coef. (kg/m <sup>3</sup> min $\mu$ molm <sup>-3</sup> s)	1.67e-005	Von Kaman constant	0.4
Min. rate of density dec. (kg/m <sup>3</sup> min)	2.3e-002	Zero velocity height (m)	3.5
Half-sat. constant for I ( $\mu$ mol/m <sup>3</sup> s)	25.	D65 (m)	0.
Half-sat. constant for N (mg/m <sup>3</sup> )	25.	Boundary rough. projection height(m)	3.e-002
Half-sat. constant for P (mg/m <sup>3</sup> )	3.	Death rate (1/d)	0.1
Reach length (m)	4840	Cross sectional area (m <sup>2</sup> )	10
Temperatue activity coefficient	1.066		
Maximum growth rate (1/s)	5.5e-005		
Gravitational acceleration (m/s <sup>2</sup> )	9.81		

Tamam iptal Uygula

Figure A5. A screenshot of the computer simulation program showing the 'Parameters' menu for the Paşaköy River, Reach 1.

The screenshot shows a software window titled 'Edit Parameters' with a tabbed interface. The 'Reach1' tab is selected, and within it, the 'Monthly Data' sub-tab is active. The window contains a table of monthly parameters for Reach 1. The parameters are Temperature (°C) and Irradiance (μmol/m²). The temperature values are: Jan (5.2), Feb (9.4), Mar (10.3), Apr (16.1), May (2.2), Jun (30), Jul (32), Aug (28), Sep (22), Oct (19), Nov (14), and Dec (11). The irradiance values are: Jan (370), Feb (143), Mar (370), Apr (315), May (370), Jun (370), Jul (370), Aug (370), Sep (370), Oct (370), Nov (370), and Dec (370). At the bottom of the window, there are three buttons: 'Tamam', 'İptal', and 'Uygula'.

Month	Temperature (°C)	Irradiance (μmol/m²)
Jan	5.2	370
Feb	9.4	143
Mar	10.3	370
Apr	16.1	315
May	2.2	370
Jun	30	370
Jul	32	370
Aug	28	370
Sep	22	370
Oct	19	370
Nov	14	370
Dec	11	370

Figure A6. A screenshot of the computer simulation program showing the 'Monthly Data' menu for thePaşaköy River, Reach 1.

Edit Parameters

Reach1 | Reach2 | Reach3 | Reach4

Variables | Parameters | Monthly Data

Initial colony depth (m)	1.	Water density (kg/m <sup>3</sup> )	1000.
Initial colony density (kg/m <sup>3</sup> )	980.	Hydraulic radius (m)	1.
Day length (min)	600.	Slope of energy gradeline	5.e-004
Ammonium concentration (mg/m <sup>3</sup> )	0.	River depth (m)	4.
Nitrite concentration (mg/m <sup>3</sup> )	6.1	Surface slope	0.96
Nitrate concentration (mg/m <sup>3</sup> )	0.8	Flow (m <sup>3</sup> /s)	2
Phosphate concentration (mg/m <sup>3</sup> )	36.7	Pre. ave. irradiance (μmol/(m <sup>2</sup> s))	38.
Initial biomass (mg/m <sup>3</sup> )	9.	External Nitrogen load (mg/m <sup>3</sup> )	100.
Cell volume / Colony volume	1.	External Phosphorus load (mg/m <sup>3</sup> )	200.
Form resistance	1.		
Colony radius (μm)	200.		

Tamam İptal Uygula

Figure A7. A screenshot of the computer simulation program showing the 'Variables' menu for the K m rl k River, Reach 1.

Edit Parameters

Reach1 | Reach2 | Reach3 | Reach4

Variables | Parameters | Monthly Data

Extinction coefficient (1/m)	2.	Manning's constant	1.
Density gain coef. (kg/(m <sup>3</sup> min))	0.132	Manning's roughness coefficient	3.e-002
Density loss coef. (kg/m <sup>3</sup> minμmolm <sup>3</sup> s)	1.67e-005	Von Kaman constant	0.4
Min. rate of density dec. (kg/m <sup>3</sup> min)	2.3e-002	Zero velocity height (m)	3.5
Half-sat. constant for I (μmol/m <sup>3</sup> s)	25.	D65 (m)	0.
Half-sat. constant for N (mg/m <sup>3</sup> )	25.	Boundary rough. projection height(m)	3.e-002
Half-sat. constant for P (mg/m <sup>3</sup> )	3.	Death rate (1/d)	0.1
Reach length (m)	2907	Cross sectional area (m <sup>2</sup> )	7.65
Temperatue activity coefficient	1.066		
Maximum growth rate (1/s)	5.5e-005		
Gravitational acceleration (m/s <sup>2</sup> )	9.81		

Tamam iptal Uygula

Figure A8. A screenshot of the computer simulation program showing the 'Parameters' menu for the Kömürlük River, Reach 1.

Edit Parameters

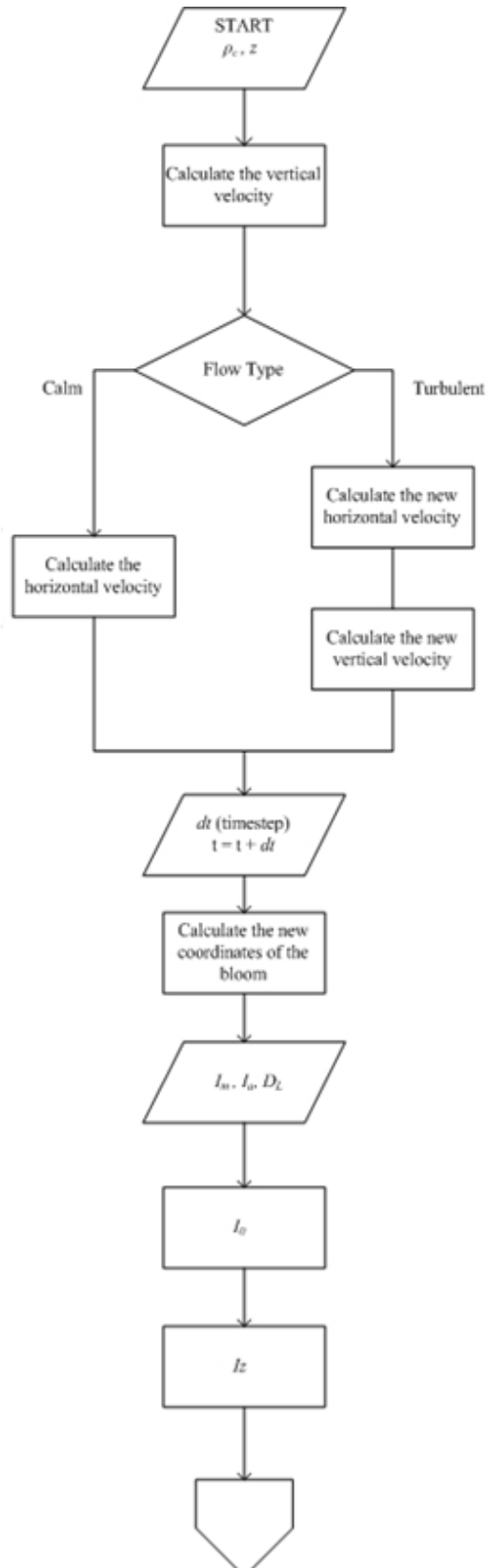
Reach1 | Reach2 | Reach3 | Reach4

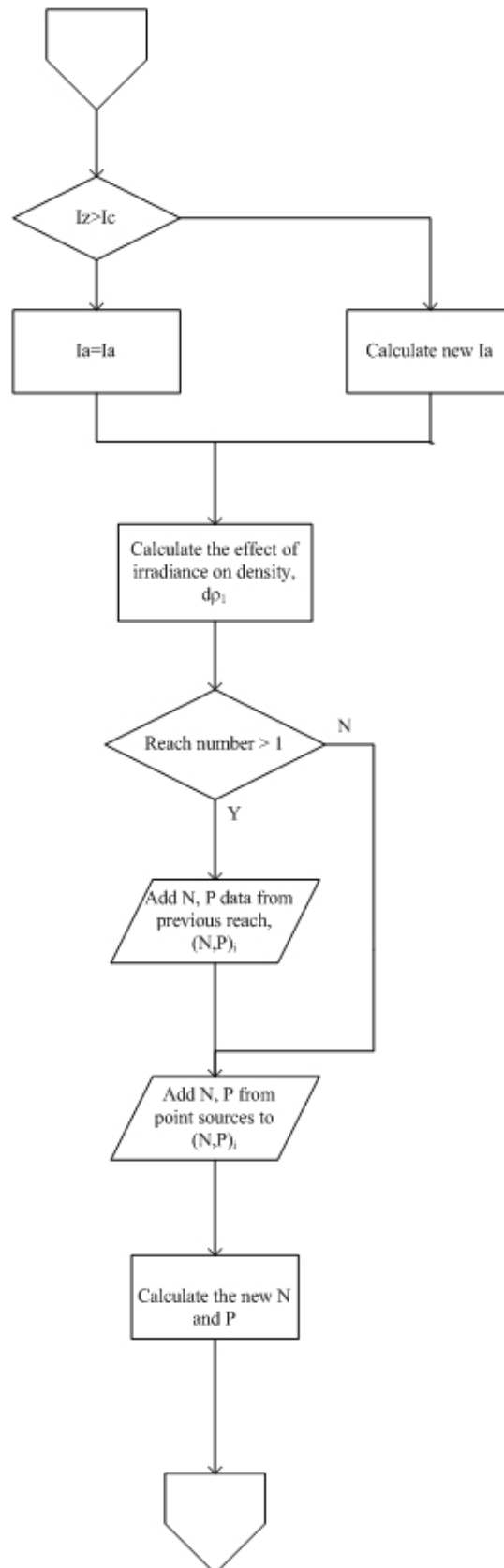
Variables | Parameters | Monthly Data

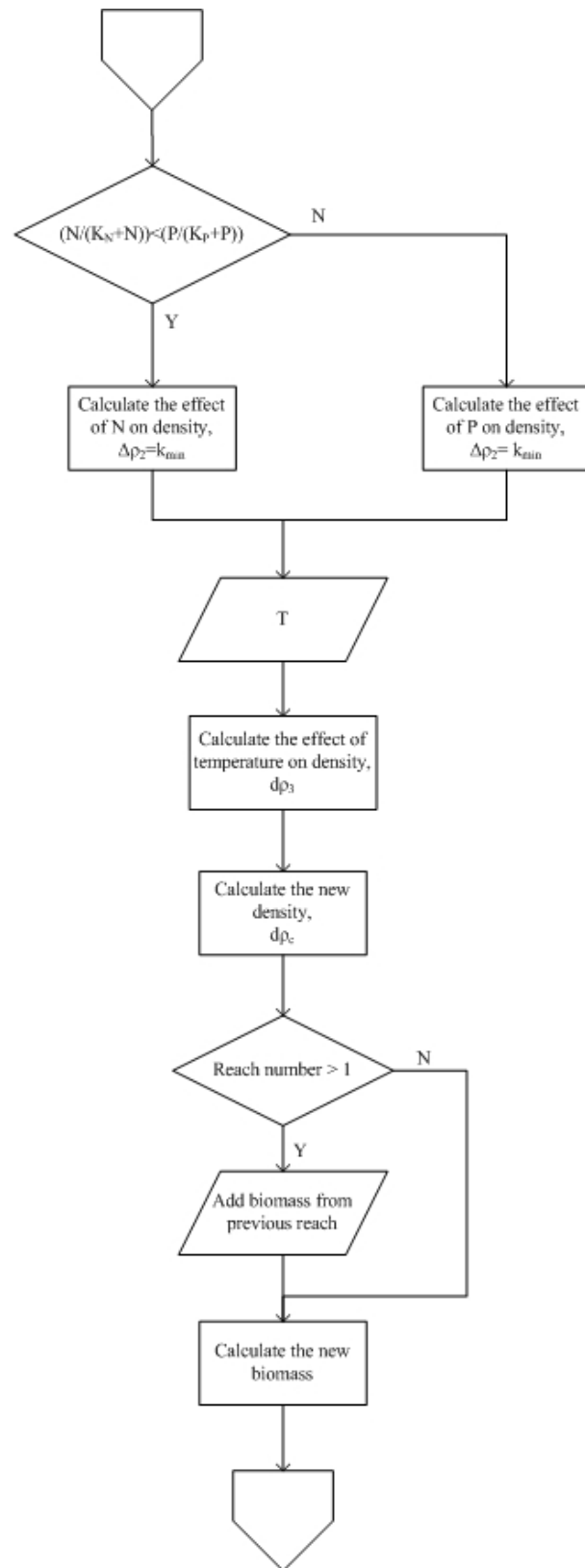
Temperature °C (Jan)	5	Irradiance $\mu\text{mol}/(\text{m}^2\text{s})$ (Jan)	370
Temperature °C (Feb)	7	Irradiance $\mu\text{mol}/(\text{m}^2\text{s})$ (Feb)	29
Temperature °C (Mar)	11	Irradiance $\mu\text{mol}/(\text{m}^2\text{s})$ (Mar)	370
Temperature °C (Apr)	12	Irradiance $\mu\text{mol}/(\text{m}^2\text{s})$ (Apr)	177
Temperature °C (May)	18	Irradiance $\mu\text{mol}/(\text{m}^2\text{s})$ (May)	370
Temperature °C (Jun)	23	Irradiance $\mu\text{mol}/(\text{m}^2\text{s})$ (Jun)	370
Temperature °C (Jul)	20	Irradiance $\mu\text{mol}/(\text{m}^2\text{s})$ (Jul)	370
Temperature °C (Aug)	22	Irradiance $\mu\text{mol}/(\text{m}^2\text{s})$ (Aug)	17
Temperature °C (Sep)	16	Irradiance $\mu\text{mol}/(\text{m}^2\text{s})$ (Sep)	370
Temperature °C (Oct)	13		
Temperature °C (Nov)	10		

Tamam İptal Uygula

Figure A9. A screenshot of the computer simulation program showing the 'Monthly Data' menu for theKömürlük River, Reach 1.

**APPENDIX B: FLOWCHART OF THE MODEL**





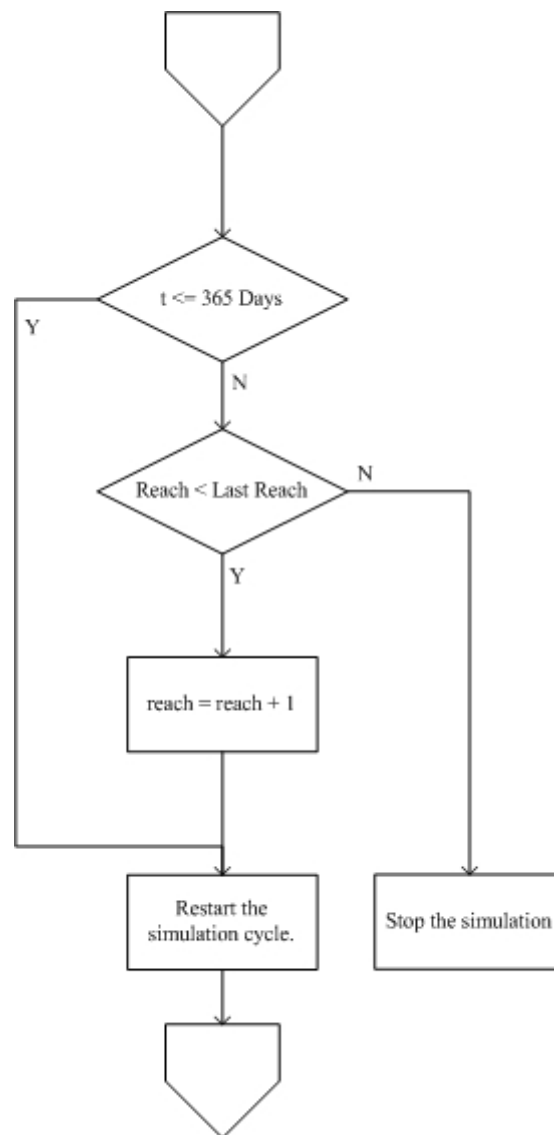


Figure B1. Flowchart of the computer simulation program.